Nonideal Multicomponent Distillation: Use of Bifurcation Theory for Design

Z. T. Fidkowski, M. F. Malone, and M. F. Doherty
Dept. of Chemical Engineering, University of Massachusetts, Amherst, MA 01003

A method for the design of distillation systems for nonideal multicomponent mixtures is described, offering an alternative to extensive performance simulations. The basis is an analysis of the pinches or "fixed points" in the model equations and the results are widely applicable because approximations such as constant volatilities and ideal solutions are unnecessary. Tangent pinches are represented naturally as turning points in the diagram of pinch composition vs. reflux ratio, giving a basis for designs that alleviate the effects of tangent pinches in certain nonideal mixtures. An efficient computational approach for design is demonstrated in examples for homogeneous liquid mixtures, containing as many as four components, with and without azeotropic behavior. The results are in excellent agreement with detailed performance simulations.

Introduction

There are important differences between design and simulation in chemical engineering, which are often ignored. In a performance evaluation (or "rating"), the inputs and all of the design parameters are given, and the objective is to calculate all of the outputs; this concept is the backbone of sequential modular simulation of chemical processes. In a design task, however, the inputs and desired outputs of the process are given, and the goal is to determine if the specifications are possible and, if so, the structure of the process flowsheet(s) and the corresponding values of the design variables necessary to achieve them.

A common and important example is the design of distillation separations. Current practice is to guess an initial design and improve it by successive simulations. For ideal mixtures, good methods are available for estimating the initial guess, such as the well known Fenske-Underwood-Gilliland method, and the performance simulation approach to process design typically works well in such cases. For nonideal mixtures, the situation is different. There are no robust methods for estimating minimum reflux or the number of stages in each column section. Nor is it possible to anticipate the presence of tangent pinches in multicomponent mixtures. For these reasons, simulators must often be run exhaustively to design a distillation system for nonideal mixtures. The only reason for the use of such an inefficient procedure is the lack of good design procedures and software tools to complement simulators.

The aim of this work is to describe a rapid and straightforward design method for nonideal, multicomponent distillation. Much of the basis for such an approach has actually been developed in previous work and consists of three main steps:

1) Checking the feasibility of the separation (Foucher et al., 1991).

2) Calculation of the minimum reflux ratio (Levy et al., 1985; Julka and Doherty, 1990).

3) Calculation of the number of theoretical stages and the distribution of nonkey components for a chosen reflux greater than the minimum and for the desired separation of the key components (Julka and Doherty, 1992).

However, a major practical limitation arises on account of the ubiquitous *tangent pitch*. We will show that this phenomenon can be easily understood as a *turning point* and that a robust and rapid design method can be developed using an arc length continuation in step 2 above.

Elementary *bifurcation* theory forms the basis for the work described here. This approach has been used widely in the analysis of transport and reaction engineering models. More recently, the performance of distillation systems has also been analyzed with this approach (for example, Kovach and Seider, 1987; Venkataraman and Lucia, 1988; Widagdo et al., 1989; Kienle and Marquardt, 1991). The main focus of this article is to study the minimum reflux and design problems, in which

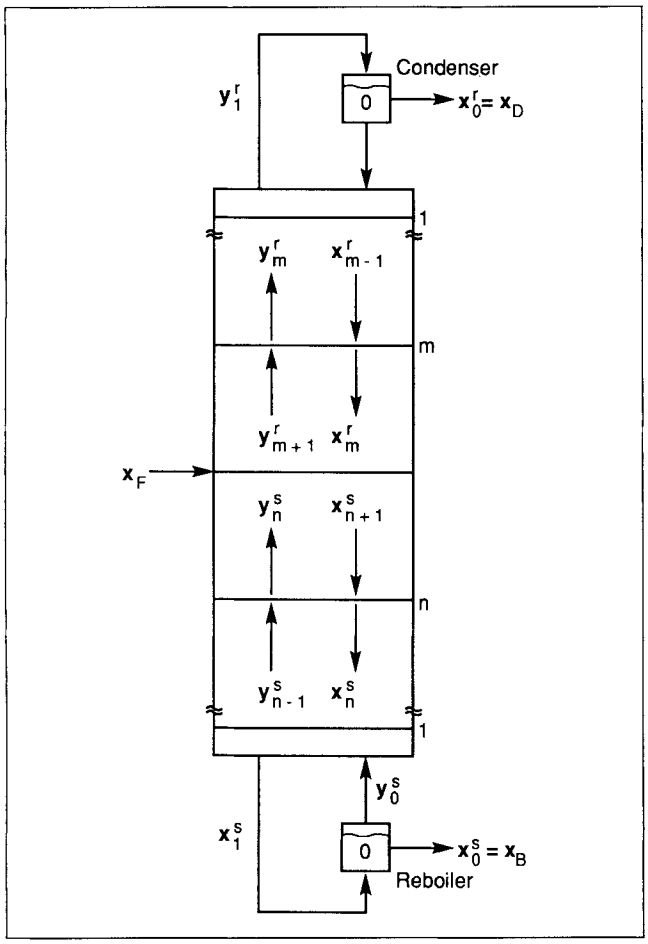

Figure 1. Simple single-feed distillation column producing two saturated liquid products.

targets for the product compositions are set in contrast to previous studies of performance models where the equipment sizes and operating conditions are specified.

Mathematical Model for a Column

The model outlined below has been proposed by Julka and Doherty (1990) for the separation of a c-component mixture in a single, conventional distillation column, with one feed stream and two product streams (Figure 1).

The following assumptions are made:

1) All stages are theoretical stages: the liquid and vapor leaving a stage are in equilibrium.

2) The process is isobaric at a known pressure.

3) There is constant molar overflow in each section of the column.

4) Both of the products are saturated liquids.

The last two assumptions are made only for simplicity of presentation and are not necessary in the method. A similar model including heat effects was described by Knight and Doherty (1986).

The overall material balance (lever rule) gives c-2 constraints on the product compositions:

$$\frac{x_{F,i}-x_{B,i}}{x_{F,1}-x_{B,1}}=\frac{x_{F,i}-x_{D,i}}{x_{F,1}-x_{D,1}} \qquad i=2,\ \ldots,\ c-1 \tag{1}$$

and the overall energy balance is:

$$s=(r+q)\frac{x_{F,1}-x_{B,1}}{x_{D,1}-x_{F,1}}+q-1 \tag{2}$$

The compositions of the liquid and vapor phases in both sections of the column are determined by the following set of difference equations. The material balance and equilibrium equations for the *rectifying profile* are:

$$x_0^r=x_D \tag{3a}$$

$$y_{j+1}^r=\frac{r}{r+1}x_j^r+\frac{1}{r+1}x_D, \quad j=0,\ 1,\ 2,\ \ldots,\ m. \tag{3b}$$

$$x_j^r=f_{\text{eq}}^{-1}(y_j^r), \quad j=1,\ 2,\ \ldots,\ m+1. \tag{3c}$$

We have similar expressions for the stripping profile:

$$x_0^s=x_B \tag{4a}$$

$$x_{j+1}^s=\frac{s}{s+1}y_j^s+\frac{1}{s+1}x_B, \quad j=0,\ 1,\ 2,\ \ldots,\ n. \tag{4b}$$

$$y_j^s=f_{\text{eq}}(x_j^s), \quad j=0,\ 1,\ 2,\ \ldots,\ n. \tag{4c}$$

The condition for a feasible column is that the profiles match at the feed stage. If stages m and n are one above and one below the feed stage, respectively, then:

$$x_{m+1}^r=x_{n+1}^s \tag{5}$$

To simplify the degrees-of-freedom analysis, we eliminate the variables corresponding to mole fractions of the internal streams for each column section from Eqs. 3 and 4:

x_0^r	from Eq. 3a	x_0^s	from Eq. 4a
$y_1^r, y_2^r, \ldots, y_{m+1}^r$	from Eq. 3b	$x_1^s, x_2^s, \ldots, x_{n+1}^s$	from Eq. 4b
$x_1^r, x_2^r, \ldots, x_{m+1}^r$	from Eq. 3c	$y_0^s, y_1^s, \ldots, y_n^s$	from Eq. 4c

There are $2(c-1)$ remaining independent equations (Eqs. 1, 2 and 5) and $[3(c-1)+5]$ variables (x_F, x_D, x_B, r, s, q, m, n), so there are $(c+4)$ degrees of freedom. After specifying the feed composition ($c-1$ variables) and its thermodynamic state (one variable), there remain 4 degrees of freedom, and only four of the $2c+2$ variables from x_D, x_B, r, s, m, n can be specified. However, not all the combinations of these variables may be chosen, for example, one cannot specify r and s independently because they are related by Eq. 2. In fact, there is one degree of freedom between r and s, and three between x_D, x_B, m, n.

Profiles and Pinches: Minimum Reflux Geometry

This topic has been discussed in some detail in previous articles (Levy et al., 1985; Julka and Doherty, 1990, 1992), and we present only a brief summary.

The mole fractions in the liquid on each stage (profiles) are

calculated by solving material balances together with equilibrium relations (Eqs. 3 and 4), starting from both ends toward the middle of the column; this is called the boundary value design procedure (BVDP). Julka and Doherty (1990) showed that solutions of Eqs. 3 and 4 exist and are unique. To calculate profiles, only Eqs. 1 through 4 are used and a distinction between the results of the BVDP and the profiles for a feasible column is necessary: Eqs. 3 and 4 always give profiles, but only some of these satisfy Eq. 5. From the overall balances, Eqs. 1 and 2, there are $(c-1)$ independent equations and $[3(c-1)+3]$ variables (x_F, x_D, x_B, r, s, q), resulting in $2(c-1)+3$ degrees of freedom. Specifying the feed composition ($c-1$ variables, x_F) and its thermodynamic state (1 variable, q) we get $[2(c-1)+3]-[c-1+1]=c+1$ degrees of freedom for the BVDP. A closer analysis shows that one can specify c product compositions (at most $c-1$ at one end of the column) and either the reflux or reboil ratio. This enables one to calculate the $c-2$ remaining product compositions from Eq. 1 and the reboil or reflux ratio from Eq. 2.

Example 1: Separation of a binary mixture

For binary mixtures, three of the four degrees of freedom for a design are $x_{D,1}$, $x_{B,1}$, and r. The composition changes can be represented as a discrete set of points (x_1, y_1) in the usual McCabe-Thiele diagram, which is shown in Figure 2 for the separation of hexane (1) and heptane (2) with the design specifications given in Table 1 (along with specifications for all subsequent examples).

Since the McCabe-Thiele representation is not possible for mixtures containing more than two components, we will represent the solutions as a set of points in a $(c-1)$-dimensional state space of liquid composition $(x_1, x_2, \ldots, x_{c-1})$. This representation of composition profiles for binary mixtures is also shown in Figure 2, by a projection of the liquid mole fractions onto the x_1 axis. The profiles start at product compositions and end at the fixed points of Eqs. 3 and 4 where the operating lines intersect the equilibrium curve. There are at least two fixed points in each profile: one a stable node and the other an unstable node. For $r<r_{min}$, the profiles are isolated from each other. At $r=r_{min}$, the stable nodes in both profiles occur at the same point. For a saturated liquid feed, this happens exactly at feed composition and for other thermodynamic states of the feed, the corresponding feed stage composition can be calculated easily. At $r>r_{min}$, the profiles overlap and we can choose an optimal feed stage location; this is the fourth degree of freedom.

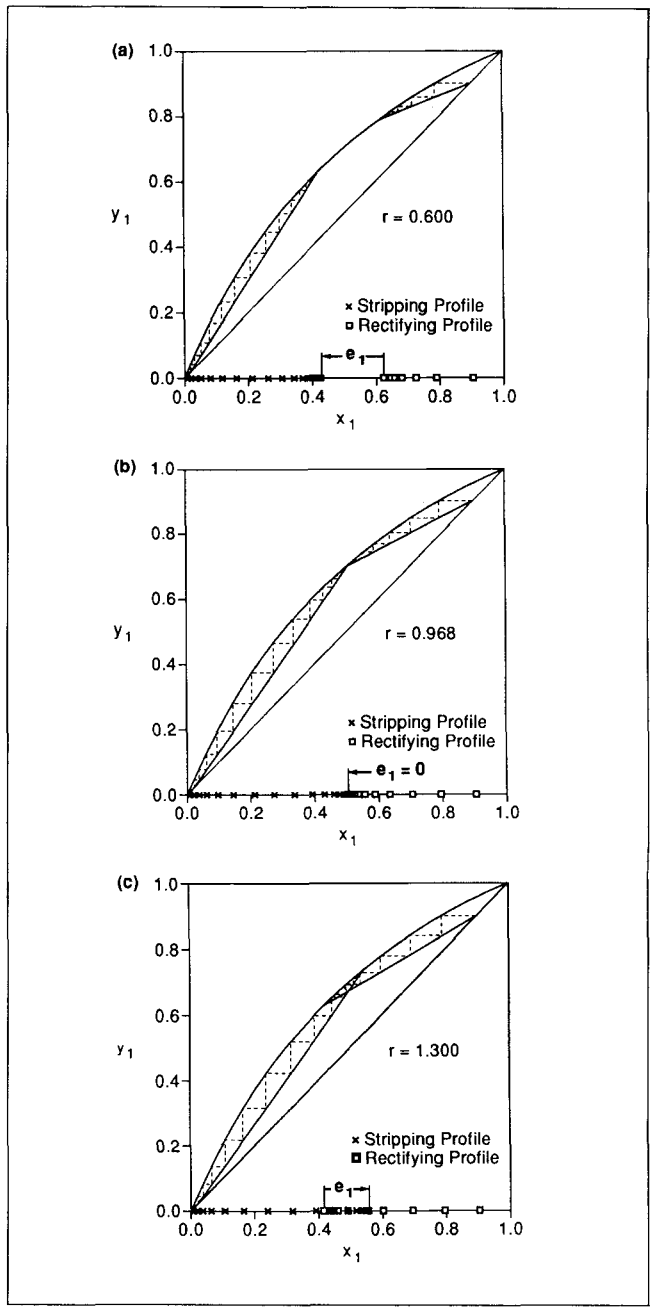

Figure 2. McCabe-Thiele diagram for a binary split (Example 1): a) $r<r_{min}$; b) $r=r_{min}$; c) $r>r_{min}$

Example 2: An ideal, ternary mixture

Liquid composition profiles for the separation of benzene from a ternary mixture of benzene (1), toluene (2) and xylene (3) (a "direct" split) are shown in Figure 3. The profiles start at the product compositions and end at the stable nodes; an additional (saddle) fixed point is present close to the binary edge in each profile. For $r<r_{min}$, the profiles do not intersect. At $r=r_{min}$, the stripping profile ends somewhere on the rectifying profile. For constant volatility mixtures and a saturated liquid feed, the stripping node, the rectifying saddle and feed composition (the points $\hat{x}^{1,s}$, $\hat{x}^{2,r}$ and x_F) are aligned at minimum reflux. In fact, the curve joining these three points is nearly linear even for many highly nonideal systems (Levy et al., 1985). For other thermodynamic states of the feed, the point x_F should be replaced by a linear combination of x_F and $\hat{x}^{1,s}$ in the alignment condition (see Julka and Doherty, 1990). At $r>r_{min}$, the profiles intersect transversely.

The four degrees of freedom chosen here are $x_{D,1}$, $x_{D,3}$, $x_{B,1}$, and r. The feed stage composition occurs at the intersection of the profiles, and the location of the feed stage is calculated by counting stages along the profiles.

This ternary picture extends to higher dimensions. The rectifying profile starts at the distillate composition and approaches $(c-2)$ saddles before ending at a stable node. A manifold of dimension $(c-2)$ is spanned by these fixed points.

Table 1. Feed and Product Purity Specifications for the Examples*

No.	Components	Feed	Specifications for Minimum Reflux: Distillate	Specifications for Minimum Reflux: Bottoms	Specifications for Design: Distillate	Specifications for Design: Bottoms	Reflux Ratio
1	1) Hexane	0.50	0.9000	0.0100			
	2) Heptane	0.50					
2	1) Benzene	0.30	0.9900	1.0E-05	0.9900	1.0E-5	
	2) Toluene	0.30					2.25
	3) Xylene	0.40	1.0E-10				
3	1) Benzene	0.50	0.9900	0.01			
	2) Ethylenediamine	0.50					
4	1) Acetaldehyde	0.30		1.0E-10			
	2) Methanol	0.30					0.87
	3) Water	0.40	1.0E-03	0.9897	1.0E-3	0.9897	
5	1) Acetone	0.30	0.74	1.0E-6	0.74	1.0E-6	1.707
	2) Methanol	0.40					1.789
	3) Water	0.30	1.0E-10				1.951
							3.352
6	1) Benzene	0.25	0.9900	1.0E-5	0.9900	1.0E-5	2.40
	2) Toluene	0.25					
	3) m-Xylene	0.25	1.0E-8				
	4) o-Xylene	0.25					

* In each case, the pressure is 1 atm, the feed is a saturated liquid and the compositions are given as mole fractions. Ideality of the vapor phase has been assumed, though this is not necessary. A range of descriptions were used for the liquid phase: a constant volatility of 2.37 was used in Example 1; in Examples 2 and 6, an ideal liquid phase (Raoult's law) was assumed; an empirical two-parameter y-x model was used in Example 3, and the activity coefficients in the liquid phase were calculated using the Margules equation for Example 4 and the Wilson equation in Example 5.

The "rectifying manifold" is linear for constant volatility systems and nearly linear for many nonideal mixtures (Julka and Doherty, 1990, 1992). The stripping profile starts at the bottoms composition and ends at the stripping node. At minimum reflux, the stripping node is located on the rectifying manifold. At a reflux ratio higher than the minimum, the stripping profile intersects the rectifying manifold transversely.

For an "indirect" split, where the heaviest component is removed in high purity, the situation is symmetrically reversed—a manifold is created by the stripping profile, the stable node in the rectifying profile ends on the stripping manifold at the minimum reboil ratio, and so on.

The fixed points in the profiles can be used to find a close approximation to the minimum reflux (or reboil) ratio *without the calculation of the intermediate profiles.* This is what makes our approach fundamentally different from simulation. The fixed points are found as the roots of the following equations:

$$\boldsymbol{F}(\hat{\boldsymbol{x}}) = \boldsymbol{0} \tag{6}$$

where $\boldsymbol{F}(\hat{\boldsymbol{x}})$ for the rectifying section is:

$$\boldsymbol{F}(\hat{\boldsymbol{x}}^r) = -\boldsymbol{y}(\hat{\boldsymbol{x}}^r) + \frac{r}{r+1}\hat{\boldsymbol{x}}^r + \frac{1}{r+1}\boldsymbol{x}_D \tag{7a}$$

and for the stripping section:

$$\boldsymbol{F}(\hat{\boldsymbol{x}}^s) = \boldsymbol{y}(\hat{\boldsymbol{x}}^s) - \frac{s+1}{s}\hat{\boldsymbol{x}}^s + \frac{1}{s}\boldsymbol{x}_B \tag{7b}$$

It is worth noting that at total reflux (reboil) Eqs. 7 become:

$$\boldsymbol{F}(\hat{\boldsymbol{x}}^r) = -\boldsymbol{y}(\hat{\boldsymbol{x}}^r) + \hat{\boldsymbol{x}}^r \tag{8a}$$

$$\boldsymbol{F}(\hat{\boldsymbol{x}}^s) = \boldsymbol{y}(\hat{\boldsymbol{x}}^s) - \hat{\boldsymbol{x}}^s \tag{8b}$$

Thus, at total reflux (reboil), *the fixed points of Eq. 6 are located at all of the pure components and azeotropes.* From Eq. 8a, we find the stability of each fixed point in the rectifying section at $r = \infty$ is the same as the stability of the corresponding pure component or azeotrope in the residue curve map (for more information about residue curve maps, see Doherty and Caldarola, 1985). From Eq. 8b, the stability of each fixed point in the stripping section at $s = \infty$ is opposite to the stability of the corresponding pure component or azeotrope in the residue curve map.

Consider a mixture without azeotropes where the components are labeled from *1* to c in the order of increasing boiling points. It is convenient to label the fixed points in the same way, according to their position at total reflux. For example, in the rectifying profile, fixed point *1* is the unstable node (lowest boiling), fixed point c is the stable node (highest boiling), and the remaining fixed points (2, 3, ..., $c-1$) are saddles (intermediate boiling). In an azeotropic mixture, depending on the distillation region where the process is performed, some azeotropes may take on the role of pure components (se Examples 4 and 5). However, the basic idea of this notation remains the same.

Julka and Doherty (1990) proposed an algebraic method for the calculation of minimum reflux ratio. For example, in a direct split one can construct the following set of vectors originating from $\hat{\boldsymbol{x}}^{2,r}$, where superscript 2,$r$ signifies fixed point number 2 in the rectifying section:

$$\boldsymbol{e}_1 = \hat{\boldsymbol{x}}^{1,s} - \hat{\boldsymbol{x}}^{2,r} \tag{9a}$$

$$\boldsymbol{e}_2 = \boldsymbol{x}_F - \hat{\boldsymbol{x}}^{2,r} \tag{9b}$$

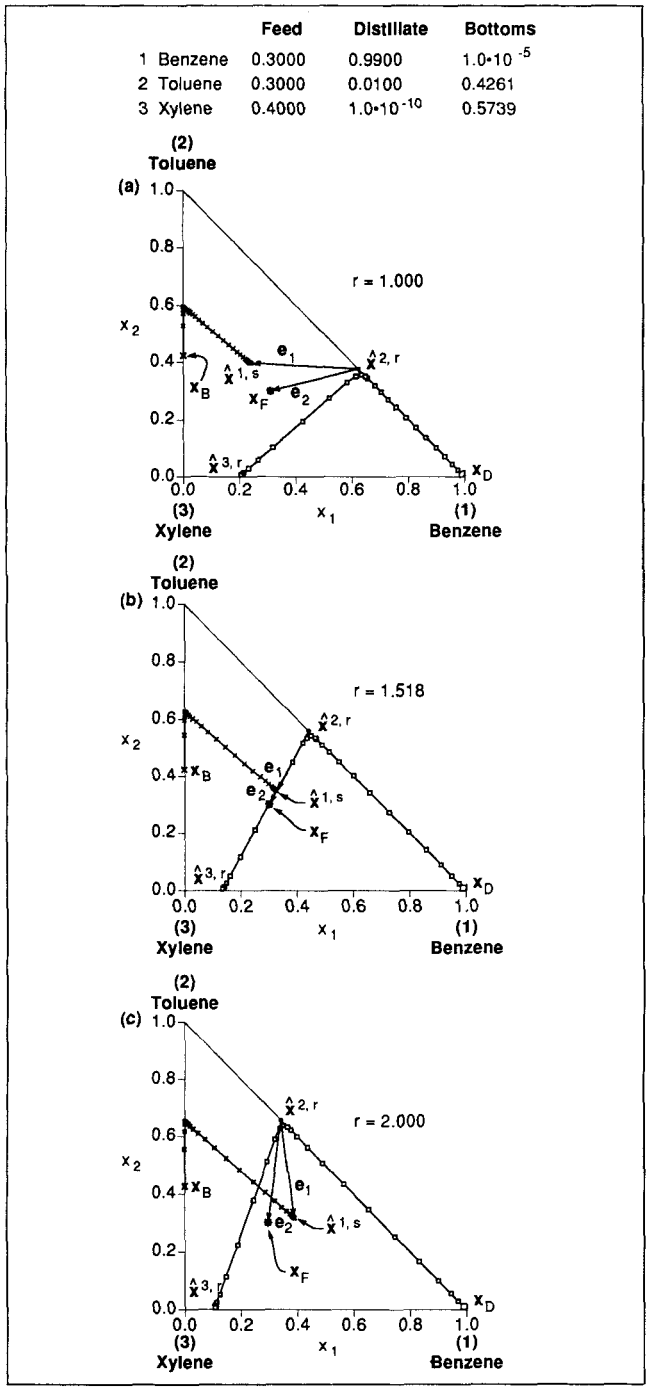

Figure 3. Liquid composition profiles for a ternary system (Example 2): a) $r < r_{min}$; b) $r = r_{min}$; c) $r > r_{min}$.

$$e_3 = \hat{x}^{3,r} - \hat{x}^{2,r} \tag{9c}$$

$$\cdots$$

$$e_{c-1} = \hat{x}^{c-1,r} - \hat{x}^{2,r} \tag{9d}$$

The minimum reflux condition is equivalent to:

$$\det[e_1, e_2, \ldots, e_{c-1}] = 0 \tag{10}$$

The meaning of the absolute value of the determinant is the following:

- For a binary mixture it is the *length* of e_1, (see Figure 2).
- For a ternary mixture it is the *area* spanned between e_1 and e_2 (see Figure 3).
- For a quaternary mixture it is the *volume* spanned by e_1, e_2, and e_3.
- For mixtures with five or more components it is a generalized "fixed point volume" defined by Eq. 10.

The method was originally developed by Julka and Doherty (1990) for quaternary mixtures and was called the "*zero volume*" method. The method is exact for constant volatility mixtures; in fact, Underwood's method can be obtained as a limiting case. For nonideal mixtures, the method is approximate though well within the accuracy of the other approximations made for design purposes.

At the minimum reflux ratio (for a direct split) the fixed points $\hat{x}^{2,r}$, ..., $\hat{x}^{c,r}$ in the rectifying profile, the feed composition x_F and the stripping node $\hat{x}^{1,s}$ (a total of $c+1$ points) are located on the same $(c-2)$-dimensional manifold. Only c of these points need to be selected to define the vectors e_1, e_2, ..., e_{c-1}, which gives c possible combinations. The origin of vectors $e(\hat{x}^{2,r}$ in Eqs. 9a-9d) might be also picked in c ways, so one can actually construct c^2 alternative *volumes*. Julka and Doherty (1990) give reasons for a selection of points according to Eqs. 9a-9d.

The *volume* (the value of the determinant defined by Eq. 10) as a function of the reflux ratio is presented in Figure 4 for Example 1 and Figure 5 for Example 2.

Equation 10 is a scalar equation in r with a supporting system of vector equations which have multiple roots for the fixed points (Eqs. 6, 7 and 9). The fixed points must be calculated before solving Eq. 10 in r; however, a value of the reflux ratio must be known to calculate the fixed points. This information loop may be torn by assuming a reflux ratio, calculating all the fixed points, classifying them (by determining which one

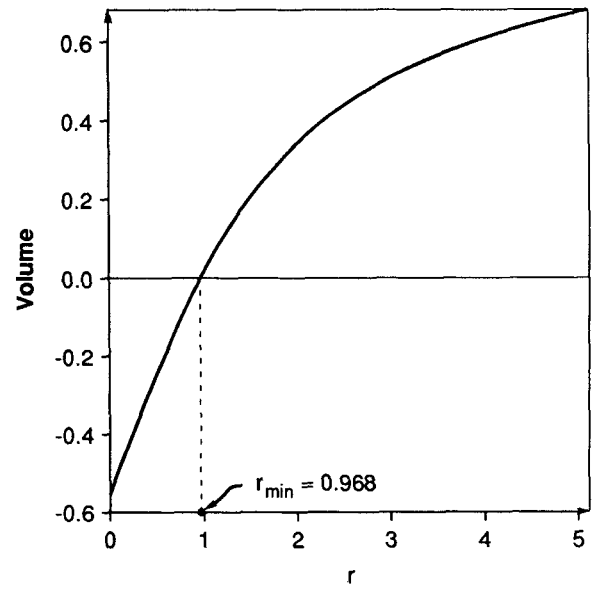

Figure 4. Volume as a function of the reflux ratio for Example 1.

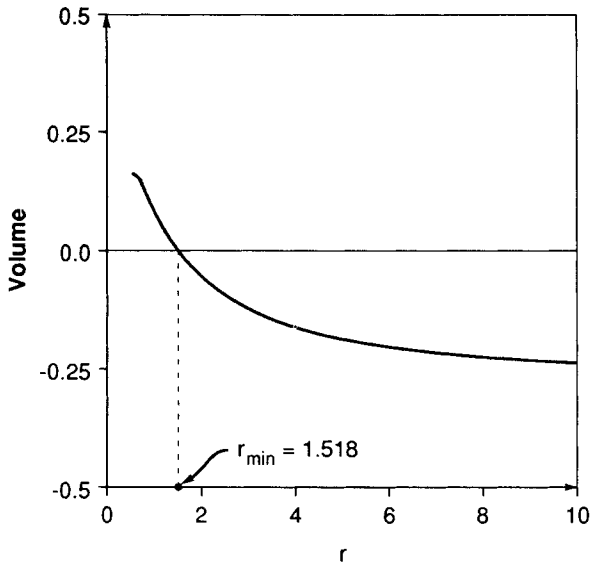

Figure 5. Volume as a function of the reflux ratio for Example 2.

is the node or the saddle with an appropriate index), and checking if Eq. 10 is satisfied. An alternative is to calculate the fixed points for all the values of the reflux ratio and then solve Eq. 10. The latter option seems to be more laborious, but we will show in the next section that it is much more useful and robust.

Tracking Fixed Points

We now discuss an algorithm for minimum reflux calculations using the "*zero volume*" method, where we seek a value of the reflux ratio that gives fixed points which satisfy the scalar equation, Eq. 10. Any systematic procedure (like secant or regula-falsi) may be used to solve the one-dimensional root-finding problem for the minimum reflux ratio, if the position of the fixed points can be calculated reliably for any value of the reflux ratio. However, many multivariable equation solvers will fail to find the fixed points unless a very good guess for $\hat{x}$ is provided. Lucia et al. (1990) have shown that conventional quasi-Newton methods for steady-state process simulations exhibit chaotic behavior with period doubling, aperiodicity and fractal basin boundaries over a wide range of starting values. Julka and Doherty (1992) obtained similar results with discontinuous or even dispersed basins of attraction for particular fixed points when solving Eq. 6.

We have found that improved performance can be obtained using continuation methods for finding fixed points. One approach is parametric continuation in which it is convenient to rewrite Eq. 6 as:

$$F(\hat{x}, \lambda) = \mathbf{0} \tag{11}$$

where

$$\lambda = \frac{1}{r} \tag{12a}$$

or

$$\lambda = \frac{1}{s} \tag{12b}$$

One can attempt to track all of the branches of fixed points originating from the pure components and azeotropes (where they are located at $\lambda = 0$), by gradually increasing the value of λ (decreasing reflux or reboil ratio), and using the most recently calculated $\hat{x}$ as an initial guess for a new point on a branch. Unfortunately, this parametric continuation also fails where the Jacobian of F becomes singular. This always happens at a *turning point* where a tangent pinch is encountered, which is a common occurrence in nonideal mixtures. Moreover, near a turning point, λ must start to decrease to follow the branch, and this requires either "hands-on" control of the algorithm or a more sophisticated approach.

The most convenient way to resolve these difficulties is to use an arc length continuation. An additional equation defining arc length (actually a pseudo arc length) is added to the system of Eqs. 11, thus

$$h(\hat{x}, \lambda, a) = 0 \tag{13}$$

If the solution is known at some point $\hat{x}(a_k)$, $\lambda(a_k)$, then a branch of solutions starting from that point can be calculated using (Keller, 1977), for example,

$$h(\hat{x}, \lambda, a) = \Theta \sum_{i=1}^{c-1} [\hat{x}_i - \hat{x}_i(a_k)] \frac{d\hat{x}_i(a_k)}{da} + (1-\Theta)[\lambda - \lambda(a_k)] \frac{d\lambda}{da} - (a - a_k) \tag{14}$$

The tuning factor Θ allows us to place different emphasis on $\hat{x}$ or λ. Actually the arc length (a) plays the role of the parameter, and λ is added to the set of unknown variables. The new system of equations may be written as follows:

$$G(\hat{x}, \lambda, a) = \begin{bmatrix} F(\hat{x}, \lambda) \\ h(\hat{x}, \lambda, a) \end{bmatrix} = \mathbf{0} \tag{15}$$

where the term in square brackets represents the augmented vector system of c equations. Equation 15 contains c unknowns ($\hat{x}_1, \hat{x}_2, \ldots, \hat{x}_{c-1}, \lambda$) and one parameter $a \geq 0$. Note that a, in contrast to λ, increases monotonically even around turning points.

The algorithm for calculating the minimum reflux ratio may be summarized as follows:

1) Solve Eq. 15 starting from each pure component and each azeotrope by arc length continuation and store the results.

2) Find the zero of the determinant (Eq. 10) using the fixed points found in step 1.

3) If there are multiple zeros of the determinant, select the one that controls to find the minimum reflux ratio.

The starting points for continuation are known exactly (pure components and azeotropes at $\lambda = 0$), and the stopping criterion is also known, when $r \to 0$. However, at values of r close to zero (in the reflux range of no physical interest), the branch of rectifying nodes approaches asymptotically close to the

branch of rectifying saddles and the continuation procedure may switch branches unpredictably. A bifurcation analysis for vanishingly small nonkey compositions gives a lower bound on the reflux ratio, where the saddle and stable node branches coalesce; at this point the continuation can be stopped. The details of this stopping criterion are somewhat technical and will be published separately.

A computer program for performing these calculations has been written. At each continuation step a Newton-Raphson method, together with an optimization of the Newton step length (Naphtali, 1964; Naphtali and Sandholm, 1971), is used to solve Eq. 15. As a result, one obtains arrays containing values of the fixed points $\hat{x}=\hat{x}(a)$ and $\lambda=\lambda(a)$ for each branch. This set of numbers serves as data for calculations of the *volume* as a function of the reflux ratio. One can also analyze the other graphs derived from these data, such as $\hat{x}$ as a function of r, or the paths of the branches in composition space. The branches of fixed points for Example 2 are shown in Figure 6. The stable node in the stripping profile (branch labeled $\hat{x}^{1,s}$) begins at the pure benzene vertex at $r=\infty$ and moves inside the triangle as r decreases. The branch of stable nodes in the rectifying profile $\hat{x}^{3,r}$ begins at the pure xylene vertex at $r=\infty$ and moves inside the triangle as r decreases, and the branch of saddles in the rectifying profile $\hat{x}^{2,r}$ begins at the pure toluene vertex and moves on a path that lies close to the benzene-toluene edge of the triangle.

Tangent Pinches

Tangent pinches are frequently encountered in nonideal mixtures (Levy and Doherty, 1986), and we begin by considering an example of tangent pinches in binary mixtures.

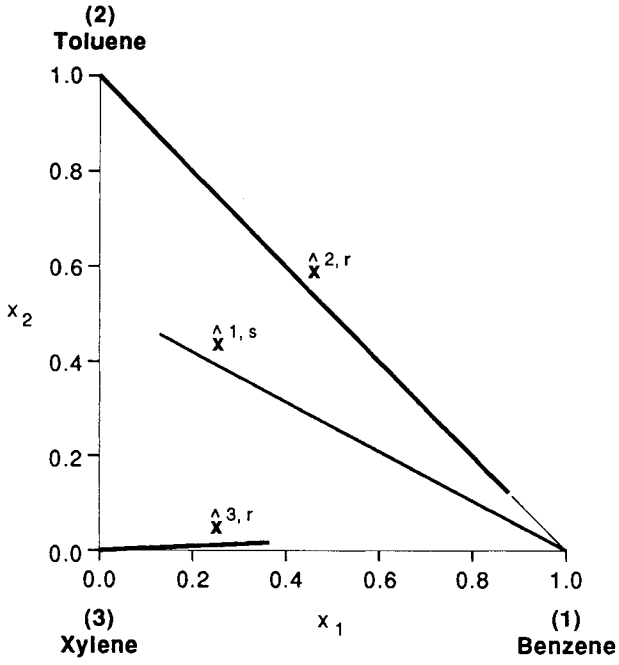

Figure 6. Branches of fixed points on the composition triangle for Example 2.

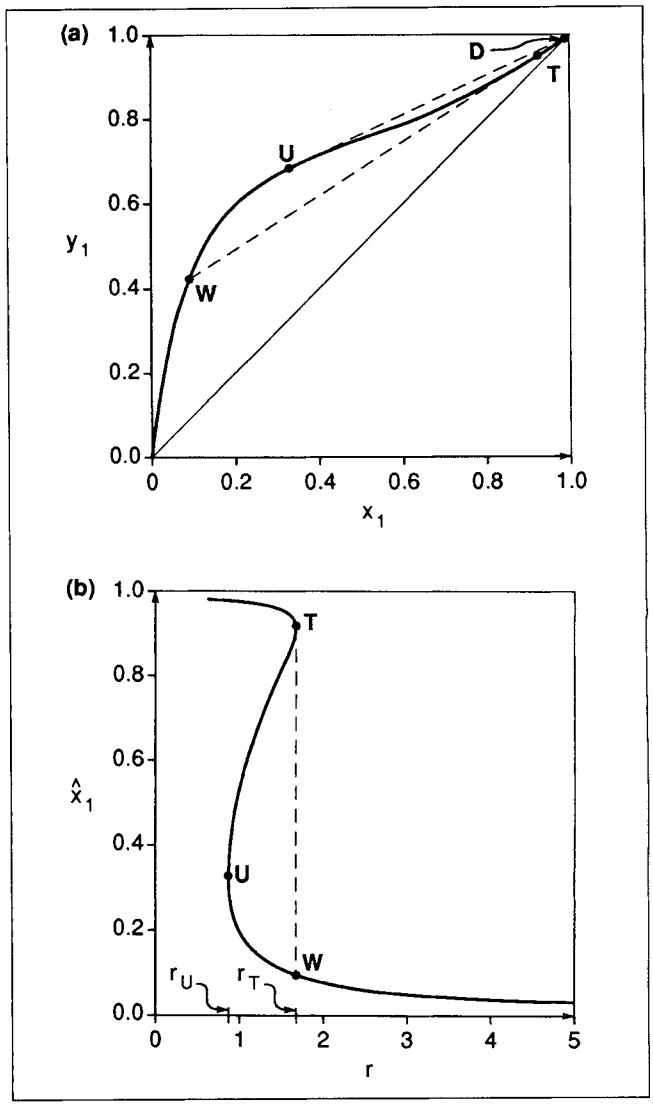

Figure 7. $y-x$ diagram for the benzene-ethylenediamine mixture at 1 atm (a) and pinch composition as a function of reflux ratio (b), corresponding to Example 3.

Example 3: a binary mixture with a tangent pinch

Figure 7a shows the vapor-liquid equilibrium and the pinch composition as a function of reflux ratio for a mixture of benzene and ethylenediamine. A tangent pinch controls the minimum reflux, and the operating line becomes tangent to the equilibrium curve. This is possible only when there is an inflection point in the equilibrium y-x relation and then only for distillate compositions rich in benzene. A branch of fixed points in the rectifying profile can be traced starting with $\lambda=0$ (total reflux) at the point (0, 0) in Figure 7a, with the reflux ratio decreasing gradually until a turning point U (in $x-\lambda$ space) is encountered. At U, the stable node changes to an unstable node, and the reflux must increase to follow the branch continuously. The unstable node changes again to a stable node at the second turning point T. Note (Figure 7b) that multiple solutions to the pinch equation, Eq. 6, exist in the region $r_U \le r \le r_T$.

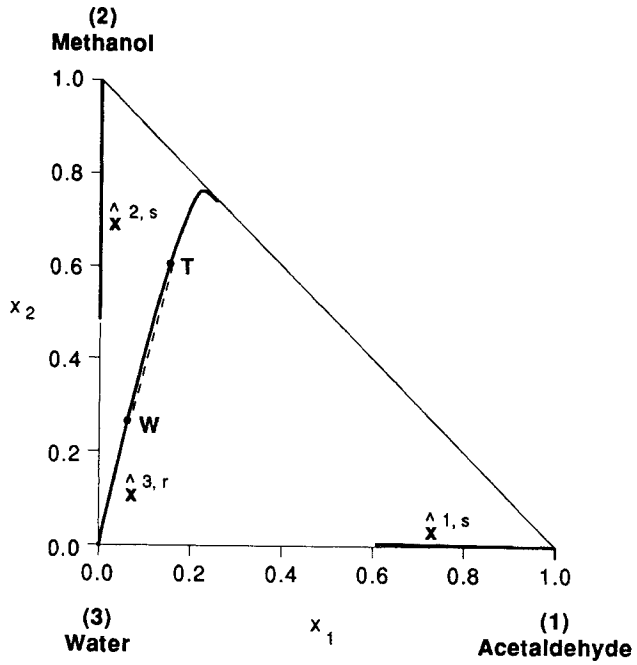

Figure 8. Branches of fixed points for Example 4.

A tangent pinch can also be calculated using bifurcation theory by rewriting Eq. 11 in terms of $\hat{x}_1$ and r, where $\hat{x}_1$ refers to the mole fraction of component 1 at a fixed point:

$$F(\hat{x}_1, r) = 0 \tag{16}$$

A necessary condition for existence of a singularity is:

$$\frac{\partial F(\hat{x}_1, r)}{\partial \hat{x}_1} = 0 \tag{17}$$

or explicitly (e.g., for the rectifying section):

$$-y_1(\hat{x}_1) + \frac{r}{r+1}\hat{x}_1 + \frac{x_{D,1}}{r+1} = 0 \tag{18}$$

$$\frac{dy_1(\hat{x}_1)}{d\hat{x}_1} = \frac{r}{r+1} \tag{19}$$

which is a system of two equations in two unknown $\hat{x}_1$ and r. These singularities correspond to either turning points or bifurcation points, which can be distinguished using higher-order conditions (e.g., Golubitsky and Schaeffer, 1985, Chap. 1). The singularities in Eqs. 18 and 19 are generally turning points as illustrated in Figure 7b. These equations normally have two solutions: one gives the reflux ratio and the mole fraction of component 1 at a tangent pinch in the rectifying section (the coordinates of point T). The other solution gives the coordinates of the (physically unattainable) point U.

The advantage of this approach is that it can be extended easily to higher dimensions. The multicomponent analogs of Eqs. 18 and 19 are:

$$-\mathbf{y}(\hat{\mathbf{x}}^r) + \frac{r}{r+1}\hat{\mathbf{x}}^r + \frac{1}{r+1}\mathbf{x}_D = \mathbf{0} \tag{20}$$

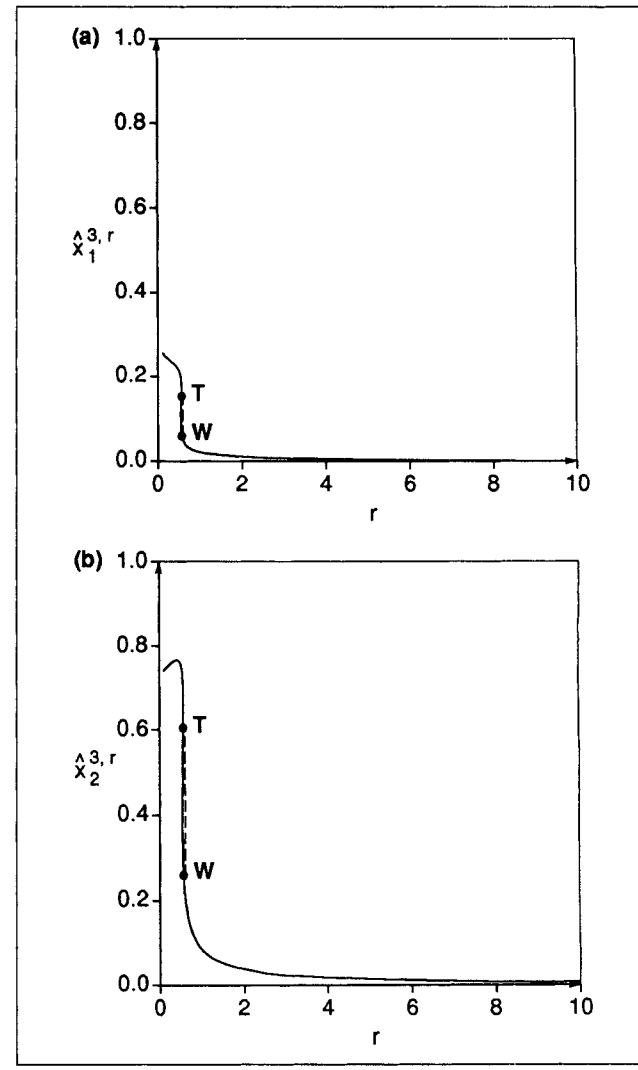

Figure 9. $\hat{x}$ vs. r diagrams showing turning points in Example 4.

$$\det\left(\mathbf{Y} - \frac{r}{r+1}\mathbf{I}\right) = \mathbf{0} \tag{21}$$

where

$$\mathbf{Y} = \left[\frac{\partial y_i}{\partial \hat{x}_j}\right]_{\hat{x}_{i \neq j}} \tag{22}$$

Doherty (1985) showed that all the eigenvalues of $\mathbf{Y}$ are strictly positive and real for mixtures with constant latent heat. At a singularity, one of these eigenvalues becomes equal to $r/(r+1)$.

Example 4: a ternary mixture with a tangent pinch

To demonstrate this formulation, we consider an indirect split of water from acetaldehyde and methanol. The branches of fixed points, the x vs. r bifurcation diagrams and composition profiles for this mixture are presented in Figures 8–10. In practice, for calculating the minimum reflux, the part of the branch from W to T is irrelevant. When the reflux ratio

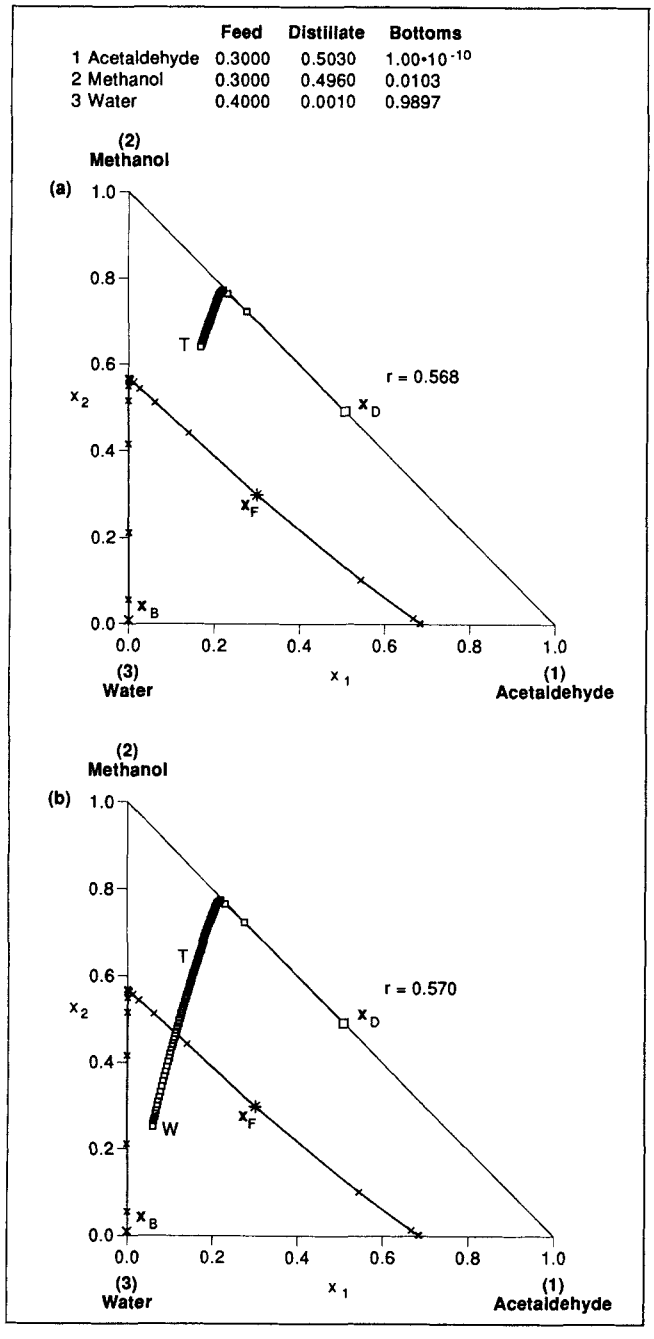

Figure 10. Liquid-phase composition profiles showing the presence of a tangent pinch in Example 4: a) $r=0.568$; b) $r=0.570$.

is changed slightly from $r=r_T$ to $r=r_T+\delta r$, there is a sudden jump of the rectifying node from point T to W as shown in Figure 10. Therefore, this part of the branch can be cut off and replaced by the dashed line TW. The branches cut in this way may be now used to calculate a modified *volume*, whose (single) zero gives the minimum reflux.

These modified *volumes* as functions of reflux ratio for Examples 3 and 4 are shown in Figures 11 and 12. It should be pointed out that if branches with turning points are not modified (cut), then their zeros will give an incorrect value for the minimum reflux ratio when the tangent pinch controls.

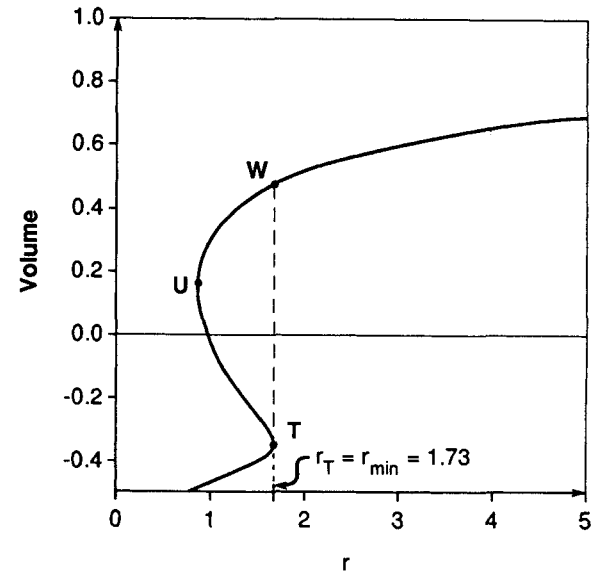

Figure 11. Volume as a function of the reflux ratio for Example 3.

One further modification to the definition of *volume* is made: if a turning point is detected on any of the branches ($\hat{x}^{1,s}$, $\hat{x}^{2,r}$, ..., $\hat{x}^{c,r}$), Eq. 9b is replaced by:

$$e_2 = \hat{x}^{c,r} - \hat{x}^{2,r} \tag{23}$$

This is one of the permissible variations of Eq. 9b as discussed by Julka and Doherty (1990) and is selected to be certain that turning points on branch $\hat{x}^{c,r}$ are included in the design procedure as process alternatives are explored, for example, if the purity specification is changing or is uncertain.

Tangent pinches correspond to turning points in one of the $\hat{x}$ vs. r bifurcation diagrams. In the Appendix, we show that

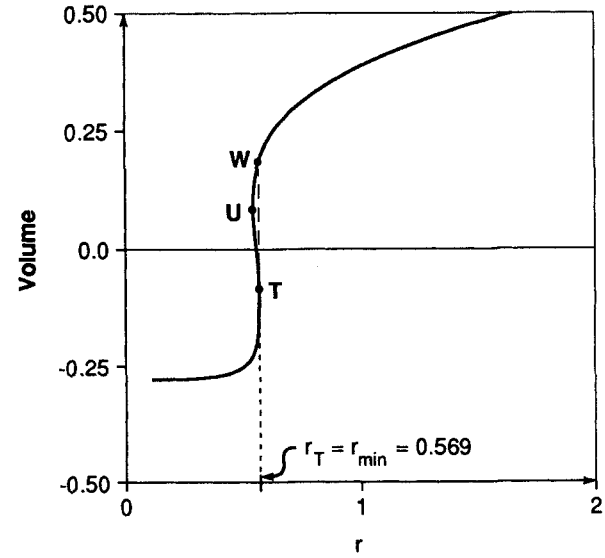

Figure 12. Volume as a function of the reflux ratio for Example 4.

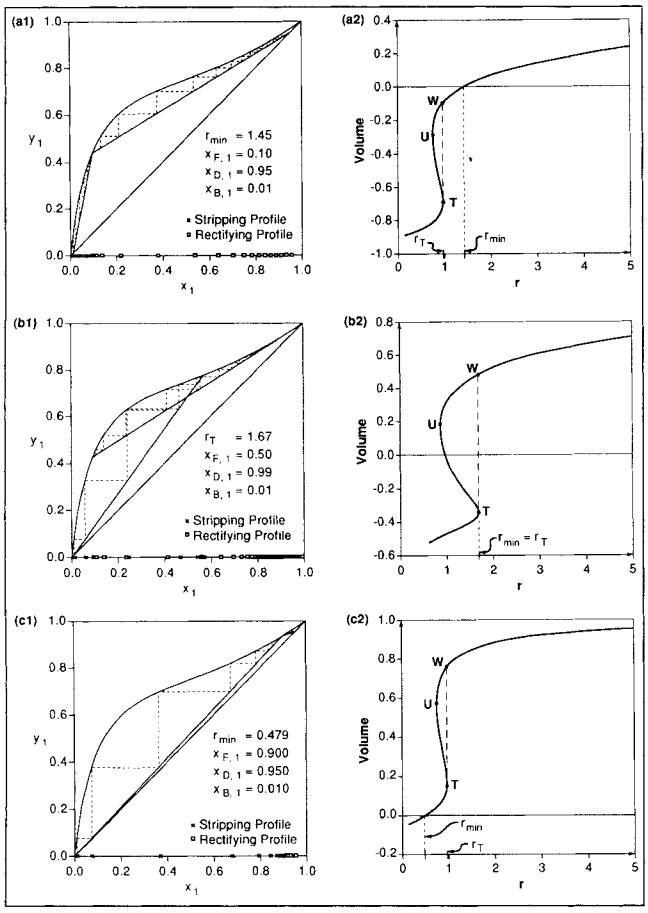

Figure 13. Three possible locations of a tangent pinch and corresponding *y-x* diagrams: a) tangent pinch at $r < r_{min}$; b) minimum reflux controlled by the tangent pinch, $r_{min} = r_T$; c) tangent pinch at $r > r_{min}$.

this also causes turning points in the *volume* vs. r diagram, which provides a more convenient representation, since *volume* is a scalar function of r. It is also worth noting that even if turning points are detected in some branches, tangent pinches do not necessarily have to control the minimum reflux, because the turning points may happen at a reflux ratio lower or higher than r_{min}. These situations are illustrated in Figure 13 for binary mixtures, where it can be seen that turning points are visible in all three cases, but that they only control minimum reflux in case b.

We know of no other published method for the treatment of tangent pinches in multicomponent mixtures, although this is essential for the solution of real problems.

Number of Stages

This design procedure is also based on the generalized geometry of profiles. It will be described here for a direct split (for the indirect split the arguments are symmetrically reversed).

Let us consider the profiles for Example 2, as shown in Figure 14. The shape of the rectifying profile depends on the distillate purity. As the amount of heavy component in the distillate is decreased, the initial portion of the rectifying profile

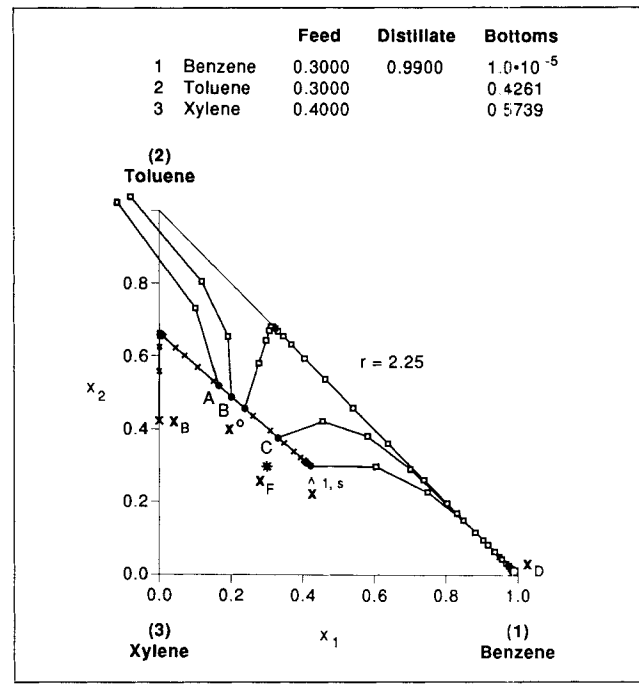

Figure 14. Liquid-phase composition profiles for Example 2.

A single stripping profile begins at x_B and several rectifying profiles begin at various points along it.

gets closer to the 1-2 edge of the composition triangle and eventually turns toward the inner part of the triangle. This corner asymptotically approaches a saddle as $x_{D,3} \to 0$.

Now suppose that one tries to compute a rectifying profile starting from various points on the stripping profile (see Figure 14). Let these points be ordered according to their arc length—the distance from the bottoms composition measured along the stripping profile. If one attempts to switch profiles too early (points A or B in Figure 14), the rectifying profile will eventually turn away from the distillate composition. Such profiles are infeasible, because they cannot reach the distillate composition even if the number of stages is infinite. The first point on the stripping profile from which a feasible rectifying profile can be drawn is denoted as x^0. One can notice that the rectifying profile beginning at x_0 will be asymptotically close to a saddle and turn along the 1-2 edge toward the distillate composition.

These ideas and the design approach can also be extended to higher dimensions (Julka and Doherty, 1990, 1992).

Feasible profiles can be drawn by beginning with a rectifying profile anywhere on the section of the stripping profile contained between x^0 and $\hat{x}^{1,s}$. For any point x in this section, the fractional distance from x^0, ω, is:

$$\omega = \frac{l(x) - l(x^0)}{l(\hat{x}_1^s) - l(x^0)} \tag{24}$$

where l is the arc length of the stripping profile in *composition space*. This is to be distinguished from a which is the arc length in λ-x space.

We can now use the following algorithm to determine the number of stages with the associated nonkey compositions in the products.

Given x_F, q and also r, $x_{D,1}$, $x_{B,1}$.

1. Calculate the reboil ratio from Eq. 2.
2. Approximate $x_{D,2} = 1 - x_{D,1}$.
3. Calculate the bottoms composition from Eq. 1.
4. Calculate the stripping profile (Eq. 4) up the the stable node ($x^{1,s}$) as a function of the arc length (l) along this profile.
5. Find the point x^0 on the stripping profile.
6. For various $\omega (0 < \omega < 1)$: a) calculate the rectifying profile; b) count the number of stages in each section; and c) store the number of stages and the distillate composition.

For a given feed composition (x_F) and thermodynamic state (q) there are 4 degrees of freedom. We specify r, $x_{D,1}$, $x_{B,1}$, ω and, in addition, assume a value for $x_{D,2}$ (so $x_{D,3}$, $x_{D,4}$ ... are equal to zero). Therefore, the problem is overspecified, and an overall material balance is generally not satisfied exactly. Nevertheless, the accuracy is usually very high since for a direct split, the compositions of heavy components in the distillate are typically in the ppm or ppb range, which we approximate as zero for the purpose of the overall mass balance. In fact, we repeated calculations for all the examples on a simulator, using the number of stages computed by this procedure and we did not notice any significant differences in composition profiles or product distribution (see the section on "Comparison with Performance Simulations"). There is also the option of repeating the design calculations from point 3 using the most recently computed distillate composition as a starting point.

The stripping profile is calculated either up to the point where the composition does not change significantly from stage to stage (close to the node) or up to a specified maximum number of stages.

The point x_0 is determined efficiently by bisection in the arc length of the stripping profile.

The number of stages and the composition of the heavy nonkey component in the distillate for Example 2 are shown in Figure 15. The number of stages in the stripping section starts at $\omega = 0$ from a finite value, increases smoothly with ω, and rises sharply to infinity as $\omega \to 1$ (where the stripping profile ends at the stable node). The number of stages in the rectifying section of the column is infinite at $\omega = 0$ (where the rectifying profile approaches asymptotically close to the saddle; see also Figure 16a) and then decreases to a finite value at $\omega = 1$ (see Figures 16b and 16c). Therefore, the curve for the total number of stages vs. ω exhibits a characteristic U shape, with both ends rising to infinity (at $\omega = 0$ and $\omega = 1$) and with a flat plateau in between, where the optimum feed tray location can be found. Some profiles for various values of ω are shown in Figure 16. The stripping profile has a sharp corner near the saddle for each ω, simply because the specification on $x_{B,1}$ remains unchanged and quite small. The sharp corner in the stripping profile disappears for larger values of $x_{B,1}$. We notice a similar sharp corner in the rectifying profile but only at small ω (where the profile goes close to the saddle). Simultaneously, the distillate contains a small amount of the heavy component at small ω, and $x_{D,3}$ increases with ω (see Figure 15b). In Figure 15a we see that the same specifications for separation of the light key component can be achieved in columns containing different number of stages in the rectifying and stripping section, while the total number of stages remains almost constant. However, the higher the number of stages in the rectifying section, the lower the amount of heavy component in the

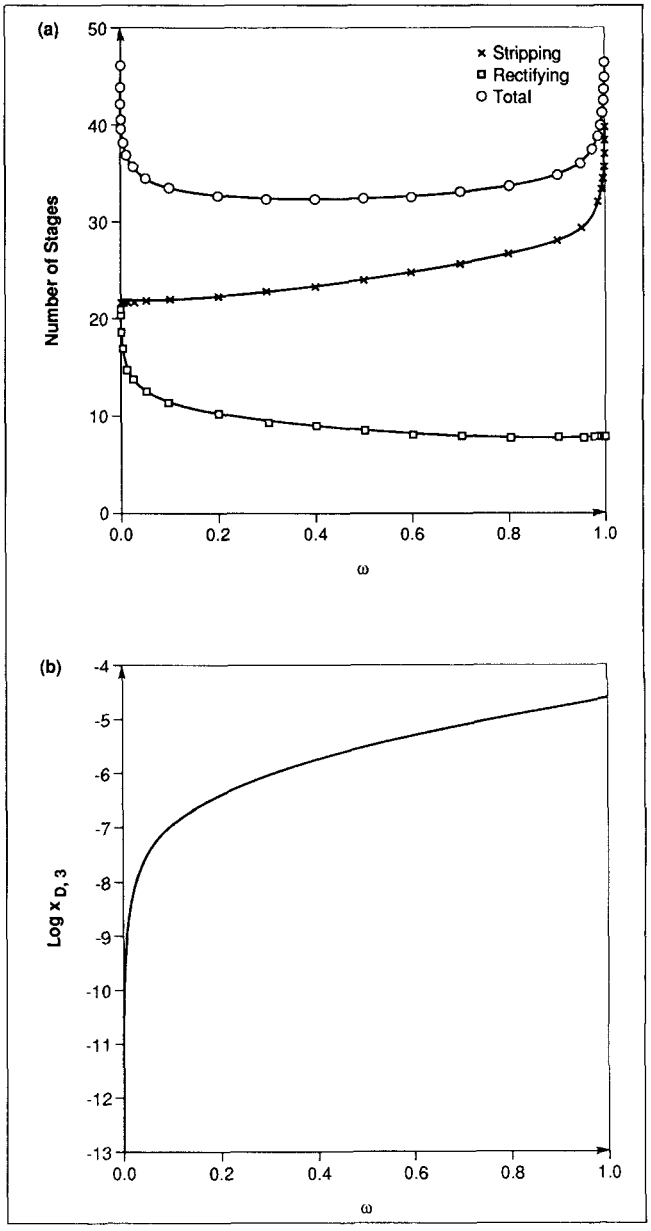

Figure 15. Number of stages (a) and distillate mole fractions of xylene, nonkey component (b), for Example 2 ($r = 2.25$).

distillate (Figure 15b). If we demand that the distillate contain extremely low amounts of the heavy component, then the number of plates in the rectifying section (and the total number of plates) increases sharply (solutions near $\omega = 0$).

The number of stages and composition of acetaldehyde, and the light nonkey component in the bottoms for Example 4 are shown in Figure 17, and the liquid composition profiles for various values of ω are shown in Figure 18. The same observations as above apply to this example also.

A computer program performing these design calculations has been written. The calculations are straightforward and quick, and the algorithm is very robust. For example, the 27 designs presented in Figure 15 were calculated in 4 seconds on a VAX Station 3100.

Next, we present two more interesting examples of designs obtained using the procedure and programs described above.

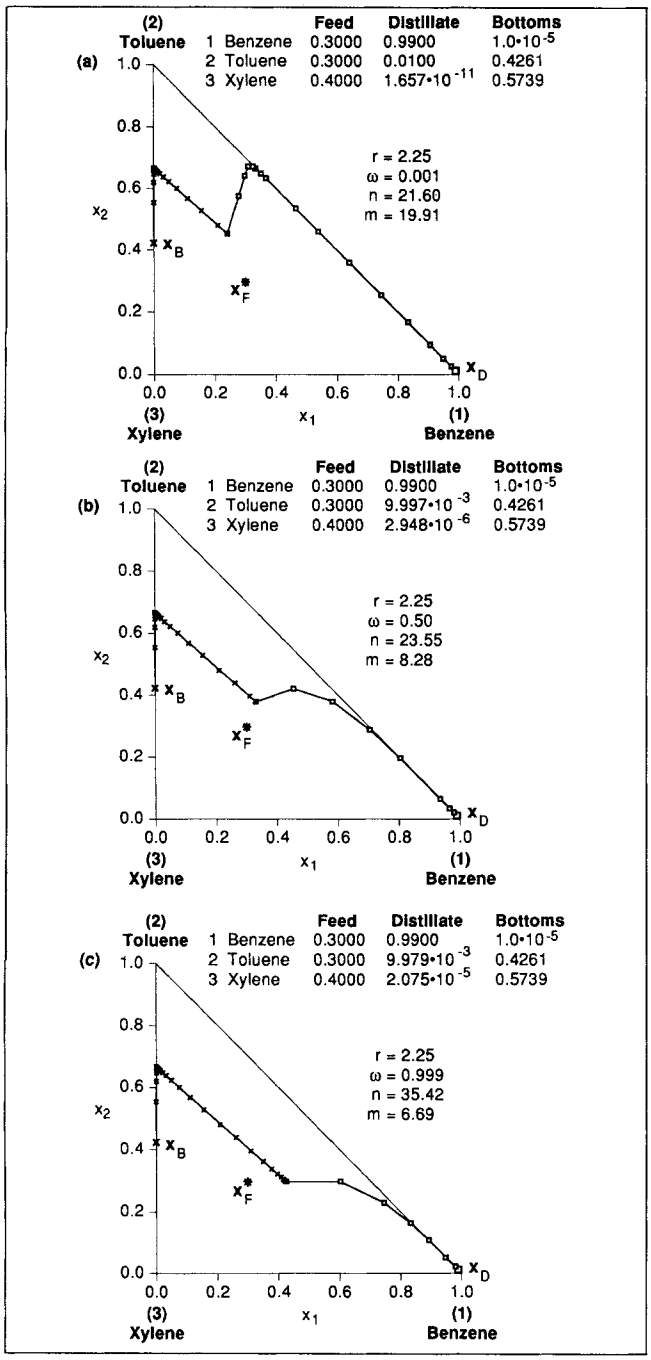

Figure 16. Liquid-phase composition profiles for various values of ω in Example 2.

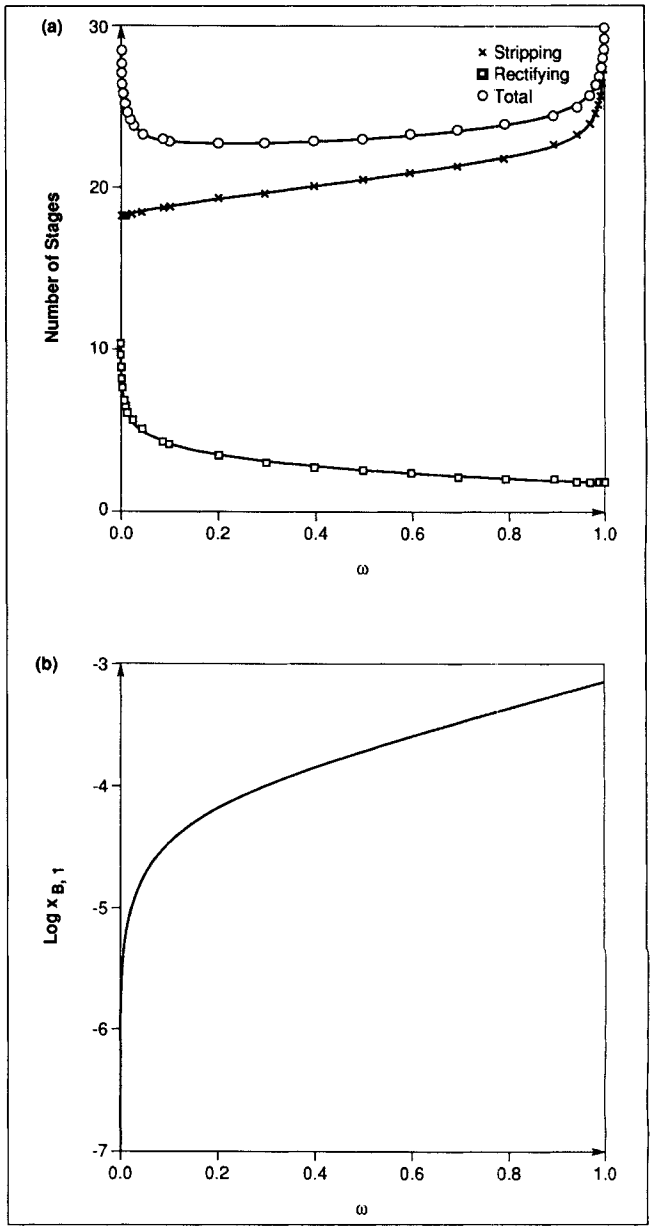

Figure 17. Number of stages (a) and bottoms mole fractions of acetaldehyde, nonkey component (b), for Example 4 ($r = 0.87$).

Example 5: a ternary azeotropic mixture with a tangent pitch

We consider the separation of an acetone-methanol azeotrope from a mixture of acetone (1), methanol (2) and water (3). This is a direct split. A branch of stripping nodes $\mathfrak{X}^{1,s}$ starts from the azeotrope A (instead of the acetone vertex) as shown in Figure 19. The branches of rectifying saddles, $\mathfrak{X}^{2,r}$, and stable nodes, $\mathfrak{X}^{3,r}$, start from the pure methanol and pure water vertices, respectively. These facts can be deduced from the residue curve map, since the stability of each fixed point in the rectifying (stripping) section at $r = \infty$ ($s = \infty$) is the same as (opposite to) the stability of the corresponding pure component or azeotrope in the residue curve map, as discussed earlier. There are turning points in two of the branches: one in the rectifying saddles $\mathfrak{X}^{2,r}$ and the other in the rectifying nodes $\mathfrak{X}^{3,r}$. The minimum reflux is controlled by a tangent pinch in rectifying profile and $r_{min} = 1.626$ as shown in Figure 20.

Designs at several reflux ratios (a total of about 220 designs) are presented in Figure 21. It takes less than 3 minutes to calculate these designs on a VAX Station 3100 using our approach. At a reflux ratio near the minimum ($r = 1.05\ r_{min}$), the total number of stages is very sensitive to ω, and the same distillate purity can be achieved in a column having 140 stages or only 40 stages depending on ω. The detrimental effects of

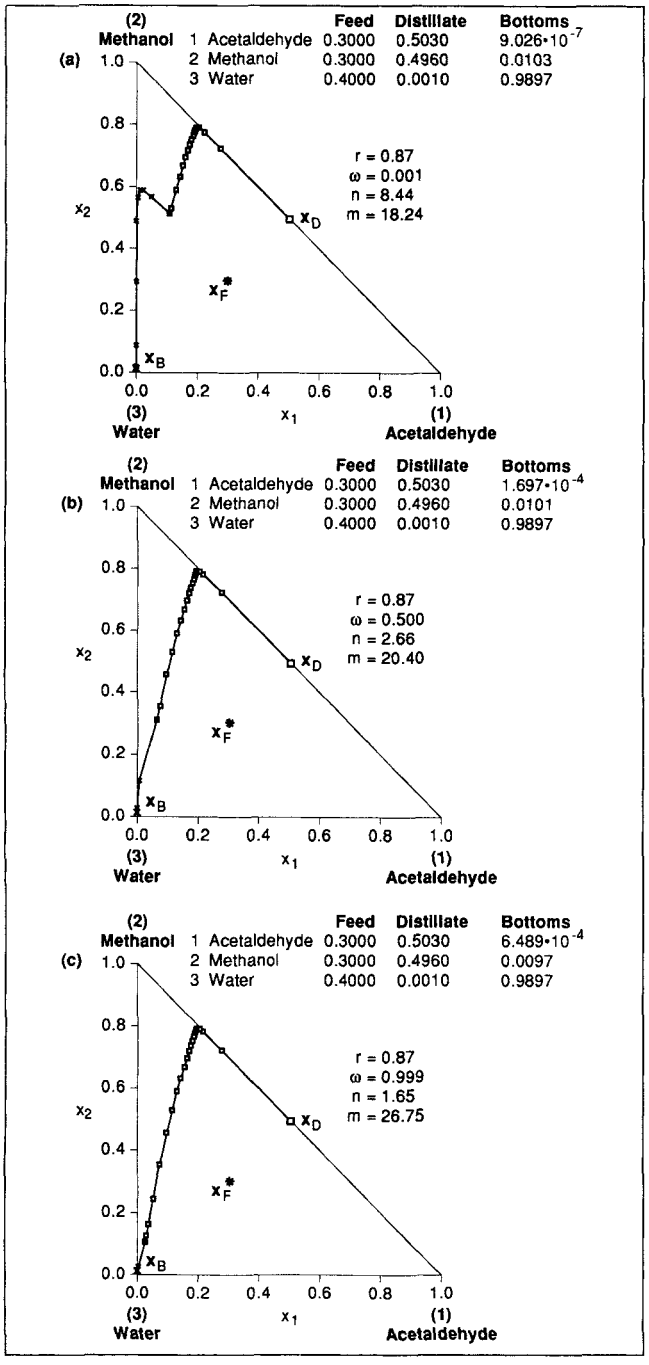

Figure 18. Liquid phase composition profiles for various values of ω in Example 4.

the tangent pinch in the rectifying section can be significantly reduced by the addition of stages in the stripping section. This is most clearly seen by comparing the profiles in Figure 22. A tangent pinch in the rectifying profile is evident in Figure 22a; the number of theoretical stages in the rectifying section can be reduced by nearly an order of magnitude by the addition of five stages in the stripping section. This eventually causes profile to approach the distillate from within the composition triangle, as shown in Figure 22c; in that 40-stage design, the distillate contains more water but the same purity of acetone. At higher reflux ratios, the number of stages does not vary

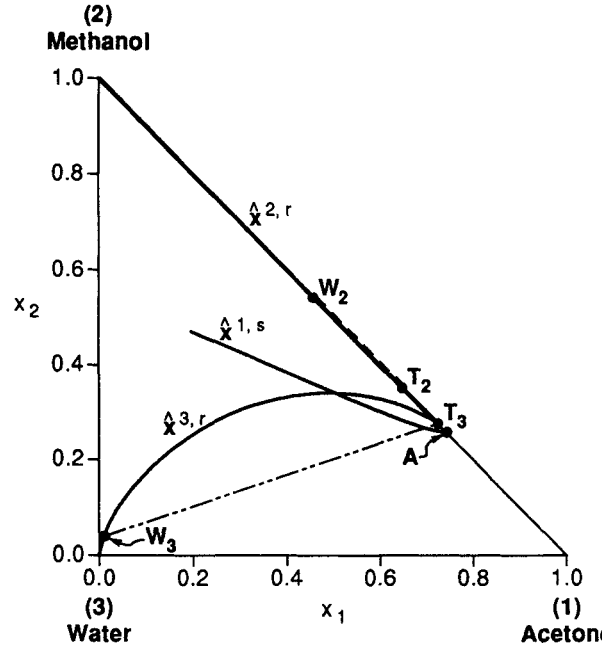

Figure 19. Branches of fixed points for Example 5.

quite so much with changes in ω and, if there is no constraint on the concentration of water in the distillate, the optimum reflux ratio should be determined.

Example 6: a quaternary ideal mixture

We examine the recovery of benzene from a mixture of benzene (1), toluene (2), *m*-xylene (3) and *o*-xylene (4). The *volume* as a function of reflux ratio is shown in Figure 23 where we see that $r_{min} = 1.667$. A spectrum of designs for $r = 2.4$ is presented in Figure 24. This example demonstrates that the procedure is not limited to binary or ternary mixtures. Al-

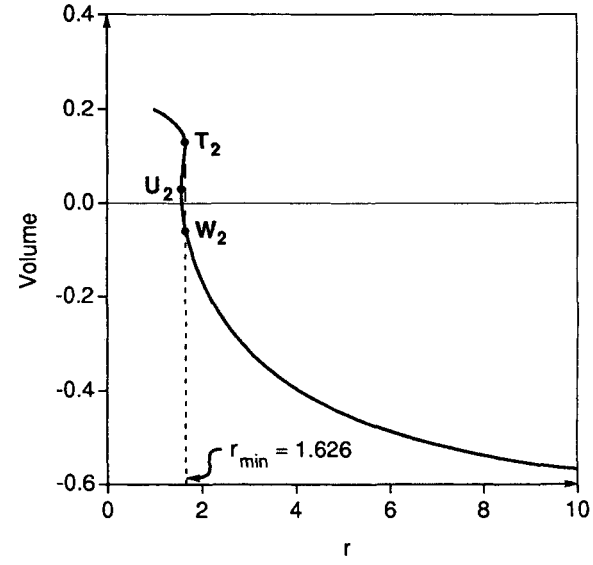

Figure 20. Volume as a function of the reflux ratio for Example 5 ($r_{min} = 1.626$).

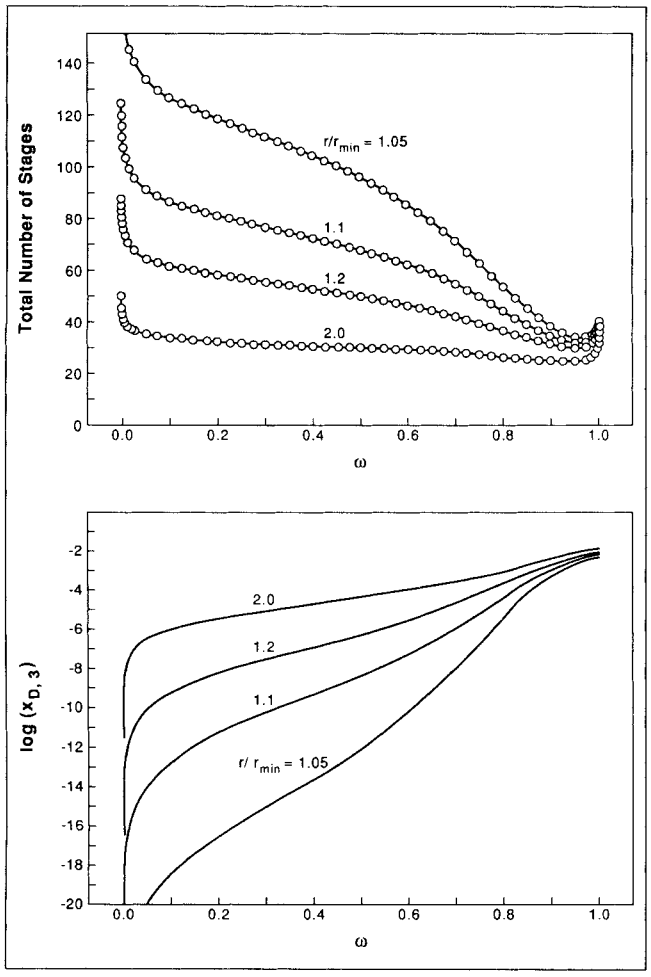

Figure 21. Number of stages (a) and distillate mole fractions of water (b) for Example 5.

though a convenient graphical representation is not available for mixtures with more than four components, the equation-based methods described in this article are applicable to such cases.

Comparison with Performance Simulations

Differences between the design approach and the performance simulations can arise for two reasons. First, there are approximations made in the design procedure as discussed in the section "Number of Stages" (especially in remark i). The second reason is connected to the fact that the number of stages calculated from the design procedure is interpolated in the usual way to find a fractional number of theoretical stages that exactly match the product specification. Of course, an integer number of stages is required for the performance model, and these were set by rounding up the fractional numbers found in the design procedure.

To assess the accuracy of our approach, many of the designs found for the examples were also used as specifications for a performance simulation to compare the temperature and composition profiles, especially for the product compositions. The designs are all computed for fixed values of the pressure, feed composition and feed quality, and with the specification of the reflux ratio and three of the product compositions. In contrast, for the performance calculation, we specify the reflux ratio, instead of the product compositions, the number of stages, the feed stage location, and the reboil ratio. This is a standard performance or "rating" calculation that can be done with most simulators.

The performance solutions were found as the steady-state limit of a dynamic model for the column. An arbitrary holdup was used on each theoretical stage, since the steady-state results are independent of these values. The performance simulations were done using the same phase equilibrium, thermodynamic

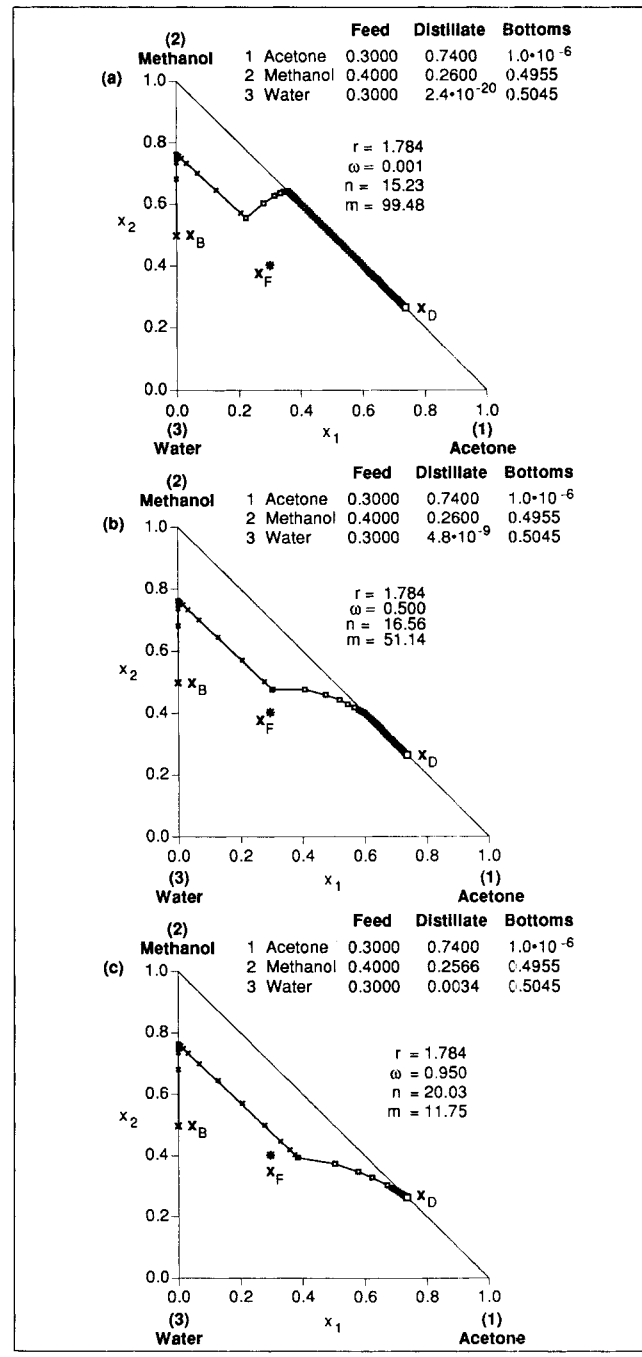

Figure 22. Liquid-phase composition profiles for various values of ω in Example 5.

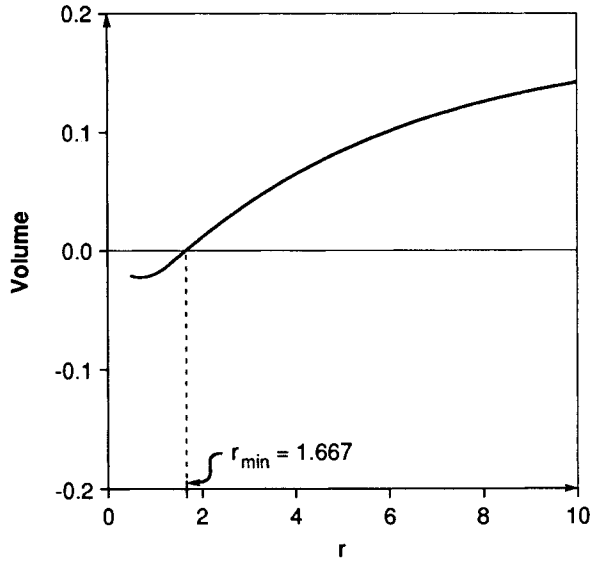

Figure 23. Volume as a function of the reflux ratio for Example 6.

models and data as the design calculations to provide a consistent comparison. The compositions and temperatures found from the design calculations were used as the initial conditions for the integration of the dynamic model, and very robust convergence behavior was found. The computation times depend on the number of stages and the number of components, but are on the order of a few minutes for a 50-stage column when using a VAX Station 3100.

Table 2 compares the results from the design procedure with the performance calculations for three of the designs represented in Figure 18 for Example 4. The mixture is nonideal but shows no azeotrope, and the separation specified in Table 1 turns out to be an indirect split in which the minimum reflux is controlled by the tangent pinch (see Figures 8, 9 and 10). The performance simulations are in excellent agreement with the design results. The largest differences are found in the stripping section, where the separation is easy, and relatively few stages are required.

Table 3 gives a similar comparison for 12 of the designs represented in Figure 21 for the azeotropic mixture from Example 5, which is a direct split with a tangent pinch. The product compositions, especially for the key components, are generally in excellent agreement, and this was also true for many other cases which were examined. The largest differences are found for reflux ratios close to the minimum and for extreme values of the feed tray location. Economics or uncertainties in the basic data generally favor designs that are a minimum of 20 to 50% above the minimum reflux ratio so that cases 7–12 in Table 3 are of practical interest. The profiles of temperature and compositions within the column for a reflux ratio 20% above the minimum and a feed tray location near the optimum (case 9 in Table 3) are shown in Figure 25. The largest differences are in the compositions found for the trace amount of the nonkey component and these are evident only because of the increased sensitivity in the logarithmic composition plot shown in Figure 25a.

The accuracy of the method for this example was typical of

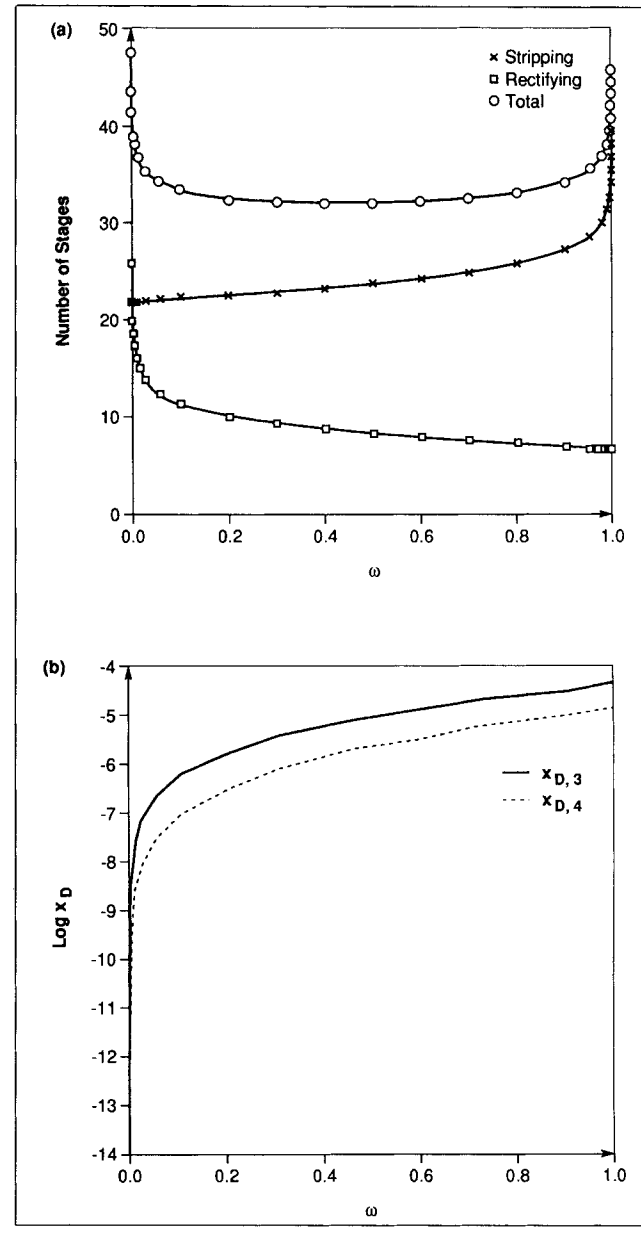

Figure 24. Number of stages (a) and distillate mole fractions of xylenes (b) in Example 6 ($r = 2.40$).

other cases studied, and it is doubtful that these differences are significant for practical purposes.

Conclusions

The design approach described above is quite general and applies to ideal and nonideal mixtures with no restrictions on the number of components. The calculations are straightforward and robust with the arc length continuation method used to solve the fixed point equations. This exploits the fact that initial conditions are known to lie at the pure components and azeotropes. A great advantage is that the method does not fail at turning points so that the design technique provides a new framework for treating tangent pinches, which can be accommodated without any special additional calculations.

Table 2. Design and Performance Results for Example 4, a Mixture of Acetaldehyde (*A*), Methanol (*M*) and Water (*W*)*

Case	r	ω	n	m	Component	Distillate Mole Fractions		Bottoms Mole Fractions	
						Design	Simulation	Design	Simulation
1	0.87	0.001	9	19	*A*	0.5030	0.5030	0.90E-6	0.38E-6
					M	0.4960	0.4962	0.0103	0.0101
					W	0.0010	0.0008	0.9897	0.9899
2	0.87	0.500	3	21	*A*	0.5030	0.5029	0.0002	0.64E-4
					M	0.4960	0.4964	0.0101	0.0098
					W	0.0010	0.0007	0.9897	0.9901
3	0.87	0.999	2	27	*A*	0.5030	0.5029	0.0006	0.0002
					M	0.4960	0.4968	0.0097	0.0090
					W	0.0010	0.0003	0.9897	0.9908

* The "zero-volume" minimum reflux ratio is 0.569 (Figure 12); the cases were chosen for a reflux ratio 50% above the minimum for small, medium and large ω, corresponding to the profiles shown in Figure 18.

Table 3. Design and Performance Results for Example 5, a Mixture of Acetone (*A*), Methanol (*M*) and Water (*W*)*

Case	r	ω	n	m	Component	Distillate Mole Fractions		Bottoms Mole Fractions	
						Design	Simulation	Design	Simulation
1	1.707	0.001	16	148	*A*	0.7400	0.7400	1.0E-6	0.66E-6
					M	0.2600	0.2600	0.4955	0.4955
					W	7.72E-28	<E-14	0.5045	0.5045
2	1.707	0.500	17	78	*A*	0.7400	0.7400	1.0E-6	.80E-6
					M	0.2600	0.2600	0.4955	0.4955
					W	2.17E-12	0.42E-12	0.5045	0.5045
3	1.707	0.950	21	14	*A*	0.7400	0.7400	1.0E-6	0.80E-6
					M	0.2576	0.2594	0.4955	0.4959
					W	0.0024	0.0006	0.5045	0.5041
4	1.784	0.001	16	100	*A*	0.7400	0.7400	1.0E-6	0.50E-6
					M	0.2600	0.2600	0.4955	0.4955
					W	1.93E-20	<E-14	0.5045	0.5045
5	1.784	0.500	17	52	*A*	0.7400	0.7400	1.0E-6	0.62E-6
					M	0.2600	0.2600	0.4955	0.4955
					W	4.77E-9	0.97E-9	0.5045	0.5045
6	1.784	0.950	21	12	*A*	0.7400	0.7400	1.0E-6	1.58E-6
					M	0.2566	0.2590	0.4955	0.4962
					W	0.0034	0.0010	0.5045	0.5038
7	1.951	0.001	15	66	*A*	0.7400	0.7400	1.0E-6	0.78E-6
					M	0.2600	0.2600	0.4955	0.4955
					W	5.51E-15	<E-14	0.5045	0.5045
8	1.951	0.500	17	34	*A*	0.7400	0.7400	1.0E-6	0.44E-6
					M	0.2600	0.2600	0.4955	0.4955
					W	6.82E-7	1.73E-7	0.5045	0.5045
9	1.951	0.950	20	10	*A*	0.7400	0.7400	1.0E-6	2.61E-6
					M	0.2550	0.2584	0.4955	0.4965
					W	0.0050	0.0016	0.5045	0.5035
10	3.252	0.001	13	30	*A*	0.7400	0.7400	1.0E-6	0.99E-6
					M	0.2600	0.2600	0.4955	0.4955
					W	1.46E-9	0.47E-9	0.5045	0.5045
11	3.252	0.500	15	16	*A*	0.7400	0.7400	1.0E-6	0.75E-6
					M	0.2600	0.2600	0.4955	0.4955
					W	4.93E-5	1.72E-5	0.5045	0.5045
12	3.252	0.950	19	6	*A*	0.7400	0.7400	1.0E-6	1.89E-6
					M	0.2526	0.2560	0.4955	0.4982
					W	0.0074	0.0040	0.5045	0.5018

* The "zero-volume" minimum reflux ratio is 1.626 (Figure 20); the cases above were chosen for a range of values in Figure 21.

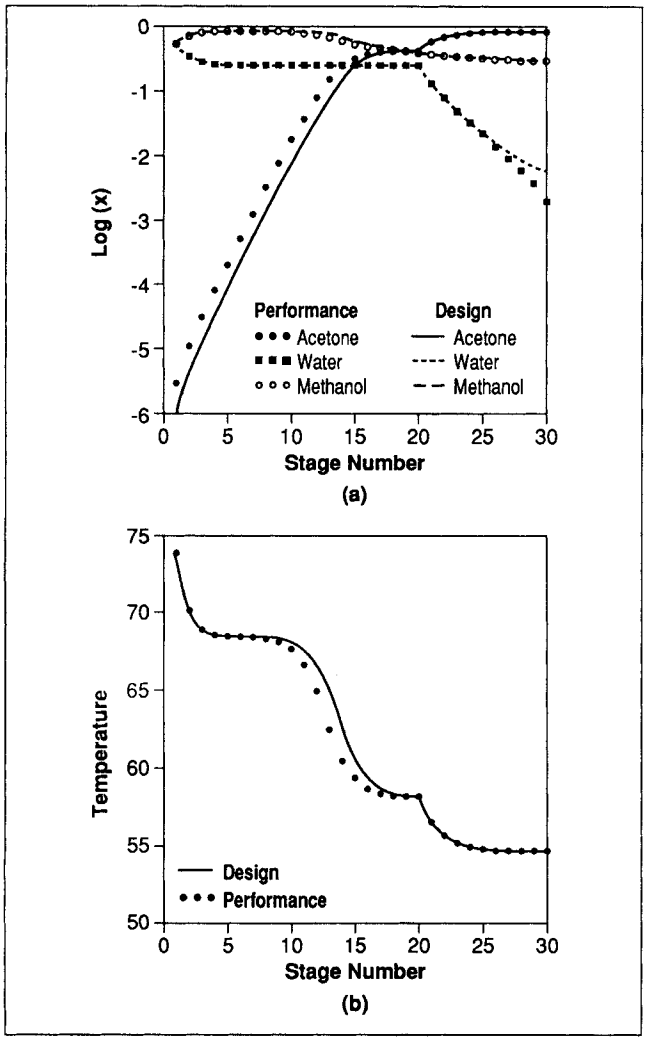

Figure 25. Design results vs. performance simulations for Example 5 using the design of Case 9 in Table 3.

Composition (a) and temperature (b) are shown for each theoretical stage in the design.

The approach is also generally much more effective for solving design problems than the common practice of using repeated application of performance calculations and trial-and-error. In contrast, the methods described here should not be used for solving rating problems in cases where they can be solved much more effectively with simulators.

Acknowledgment

We are grateful for financial support from E. I. duPont Co. and Eastman Kodak Co. We also acknowledge Vivek Julka for his helpful suggestions.

Notation

a = arc length of fixed points branch in $x-\lambda$ space
c = number of components
e = vector defined by Eqs. 9a-9d
f_{eq} = equilibrium relation
F = $[F_1, F_2, \ldots, F_{c-1}]^T$, vector function
G = $[G_1, G_2, \ldots, G_c]^T$, vector function
h = scalar function defined by Eq. 14
I = identity matrix
l = arc length of a profile in composition space
log = 10 base logarithm
m = number of stages in the rectifying section
n = number of stages in the stripping section
q = thermodynamic state of the feed
r = reflux ratio
s = reboil ratio
x = mole fraction in the liquid phase
x = $[x_1, x_2, \ldots, x_{c-1}]^T$, vector of mole fractions in the liquid phase
$\hat{x}$ = $[\hat{x}_1, \hat{x}_2, \ldots, \hat{x}_{c-1}]^T$ liquid composition of a fixed point
y = mole fraction in the vapor phase
y = $[y_1, y_2, \ldots, y_{c-1}]^T$, vector of mole fractions in the vapor phase
Y = matrix of derivatives of y with respect to x

Greek letters

Θ = tuning factor in Eq. 14
λ = defined by Eq. 12
ω = fractional distance of points $x-x^0$ defined by Eq. 24

Subscripts

B = bottoms
D = distillate
F = feed
i = component
j = stage
k = point on a branch
min = minimum
T = tangent pinch

Superscripts

r = rectifying section
s = stripping section
T = transpose
1, 2, ... c = labeling of fixed points
0 = intersection of profiles for $\omega=0$

Literature Cited

Doherty, M. F., "Properties of Liquid-Vapor Composition Surfaces for Multicomponent Mixtures with Constant Latent Heat," *Chem. Eng. Sci.*, **40**, 1979 (1985).

Doherty, M. F., and G. A. Caldarola, "Design and Synthesis of Homogeneous Azeotropic Distillations: 3. The Sequencing of Columns for Azeotropic and Extractive Distillations," *I&EC Fundam.*, **24**, 474 (1985).

Foucher, E., M. F. Malone, and M. F. Doherty, "Automatic Screening of Entrainers in Homogeneous Azeotropic Distillation," *Ind. Eng. Chem. Res.*, **29**, 760 (1991).

Golubitsky, M., and D. G. Schaeffer, *Singularities and Groups in Bifurcation Theory*, Vol. 1, Springer-Verlag, New York (1985).

Julka, V., "A Geometric Theory of Multicomponent Distillation," PhD Thesis, Univ. of Massachusetts, Amherst (1992).

Julka, V., and M. F. Doherty, "Geometric Behavior and Minimum Flows for Nonideal Multicomponent Distillation," *Chem. Eng. Sci.*, **45**, 1801 (1990).

Julka, V., and M. F. Doherty, "Geometric Nonlinear Analysis of Multicomponent Nonideal Distillation: a Simple Computer—Aided Design Procedure," *Chem. Eng. Sci.*, in press (1992).

Kienle, A., and W. Marquardt, "Bifurcation Analysis and Steady-State Multiplicity of Multicomponent Nonequilibrium Distillation Processes," *Chem. Eng. Sci.*, **46**, 1757 (1989).

Keller, H. B., "Numerical Solution of Bifurcation and Nonlinear Eigenvalue Problems," *Applications of Bifurcation Theory*, P. H. Rabinowitz, ed., Academic Press, 359 (1977).

Knight, J. R., and M. F. Doherty, "Design and Synthesis of Homogeneous Azeotropic Distillations: V. Columns with Nonnegligible Heat Effects," *Ind. Eng. Chem. Fundam.*, **25**, 279 (1986).

Kovach III, J. W., and W. D. Seider, "Heterogeneous Azeotropic Distillation Homotopy Continuation Methods," *Comp. Chem. Eng.*, **11**, 593 (1987).
Levy, S. G., D. B. Van Dongen, and M. F. Doherty, "Design and Synthesis of Homogeneous Azeotropic Distillations: II. Minimum Reflux Calculations for Nonideal and Azeotropic Columns," *Ind. Eng. Chem. Fundam.*, **24**, 463 (1985).
Levy, S. G., and M. F. Doherty, "A Simple Exact Method for Calculating Tangent Pinch Points in Multicomponent Nonideal Mixtures by Bifurcation Theory," *Chem. Eng. Sci.*, **41**, 3155 (1986).
Lucia A., X. Guo, P. J. Richey, and R. Derebail, "Simple Process Equations, Fixed Point Methods, and Chaos," *AIChE J.*, **36**, 641 (1990).
Naphtali, L. M., "Process Heat and Material Balances," *Chem. Eng. Prog.*, **60** (9), 70 (1964).
Naphtali, L. M., and D. P. Sandholm, "Multicomponent Separation Calculations by Linearization," *AIChE J.*, **17**, 148 (1971).
Seydel, R., "From Equilibrium to Chaos—Practical Bifurcation and Stability Analysis," Elsevier, New York (1988).
Venkataraman, S., and A. Lucia, "Solving Distillation Problems by Newton-Like Methods," *Comp. Chem. Eng.*, **12**, 55 (1988).
Widagdo, S., W. D. Seider, and D. H. Sebastian, "Bifurcation Analysis in Heterogeneous Azeotropic Distillation," *AIChE J.*, **35**, 1457 (1989).

Appendix

We derive sufficient conditions for a turning point in one of the elements, say, $\hat{x}_i$ vs. r, of the fixed point branch, $\hat{\boldsymbol{x}}(r)$, to imply that all the other elements, $\hat{x}_k$ vs. r, $k=1, 2, c-1$, also exhibit a turning point at the same value of r. We also derive conditions which guarantee that a turning point on a branch of fixed points implies that in the *volume* vs. r graph. Proofs are presented for ternary mixtures, but can be extended easily to multicomponent mixtures.

The fixed point equation for the rectifying section (Eqs. 6 and 7a) may be rewritten as:

$$F(\hat{x}) = -y + \frac{r}{r+1}\hat{x} + \frac{1}{r+1}x_D = 0 \tag{A1}$$

Note that if for any component i, $y_i = \hat{x}_i$, then $y_i = x_{D,i}$ for each $r \geq 0$. Circumstances that give rise to the case $y_i = \hat{x}_i$ include the instances: whenever the distillate is specified as (1) a pure component ($x_{D,1}=1$, $x_{D,j}=0$, $j=2,\ldots,c$), (2) an azeotrope, or (3) when $x_{D,1}+x_{D,2}=1$, $x_{D,j}=0$, $j=3,\ldots,c$. Excluding these limiting cases from further consideration we can rearrange Eq. A1 as follows:

$$r = -\frac{y_i - x_{D,i}}{y_i - \hat{x}_i},\ i=1, 2. \tag{A2}$$

For fixed distillate composition, the right side of Eq. A2 is a function of the liquid composition at the fixed point. Denoting this function as $\Phi = [\phi_1, \phi_2]^T$, we obtain the following set of equations describing a curve in $\boldsymbol{x}$-r space:

$$r = \phi_1(\hat{\boldsymbol{x}}) = \phi_2(\hat{\boldsymbol{x}}) \tag{A3}$$

or equivalently

$$r\mathbf{1} - \Phi(\hat{\boldsymbol{x}}) = \mathbf{0} \tag{A4}$$

where $\mathbf{1}$ represents a column vector with each of its elements equal to unity. Differentiating Eq. A4 we get the following constraint on $d\hat{\boldsymbol{x}}$ along a branch of roots:

$$\mathbf{1}dr = \boldsymbol{J}_\phi d\hat{\boldsymbol{x}} \tag{A5}$$

The Jacobian of Φ is written as:

$$\boldsymbol{J}_\phi = \begin{bmatrix} \phi_{1,1} & \phi_{1,2} \\ \phi_{2,1} & \phi_{2,2} \end{bmatrix} \tag{A6}$$

and by differentiating Eq. A2 we obtain:

$$\boldsymbol{J}_\phi = \begin{bmatrix} \dfrac{\hat{x}_1 - x_{D,1}}{(y_1 - \hat{x}_1)^2} & 0 \\ 0 & \dfrac{\hat{x}_2 - x_{D,2}}{(y_2 - \hat{x}_2)^2} \end{bmatrix} \begin{bmatrix} y_{1,1} - \dfrac{y_1 - x_{D,1}}{\hat{x}_1 - x_{D,1}} & y_{1,2} \\ y_{2,1} & y_{2,2} - \dfrac{y_2 - x_{D,2}}{\hat{x}_2 - x_{D,2}} \end{bmatrix} \tag{A7}$$

Using Eq. A2 to simplify the nondiagonal matrix, we find that the Jacobian is the product of a diagonal matrix (A), and the matrix $\{Y - [r/(r+1)]I\}$ (see also Eq. 21):

$$\boldsymbol{J}_\phi = \boldsymbol{A}\left(\boldsymbol{Y} - \frac{r}{r+1}\boldsymbol{I}\right) \tag{A8}$$

Since we have excluded the case $y_i = \hat{x}_i$, it follows that $x_i \neq x_{D,i}$, and the elements of the diagonal matrix $\boldsymbol{A}$ are nonzero. Therefore, the determinant of $\boldsymbol{J}_\phi$ is zero, only if one of the eigenvalues of matrix $\boldsymbol{Y}$ is equal to $r/(r+1)$, and consequently, a singularity in one of the branches implies that $\det(\boldsymbol{J}_\phi) = 0$.

From Eqs. A5 and A6 we have:

$$(\phi_{1,1} - \phi_{2,1})d\hat{x}_1 = -(\phi_{1,2} - \phi_{2,2})d\hat{x}_2 \tag{A9}$$

At a turning point on a $\hat{\boldsymbol{x}}-r$ branch the terms in brackets of Eq. A9 can be shown to be nonzero, since the vector $\mathbf{1}$ in Eq. A5 cannot be contained in the column space of matrix $\boldsymbol{J}_\phi$ (see also Seydel, 1988, p. 59).

Introducing Eq. A9 in Eq. A5 we obtain:

$$\frac{dr}{d\hat{x}_1} = -\frac{\det \boldsymbol{J}_\phi}{(\phi_{1,2} - \phi_{2,2})} \tag{A10}$$

$$\frac{dr}{d\hat{x}_2} = \frac{\det \boldsymbol{J}_\phi}{(\phi_{1,1} - \phi_{2,1})} \tag{A11}$$

The last two equations prove that if a branch turns in $r-\boldsymbol{x}$ space, the turning point is visible in both its projections, that is, in $r-x_1$ and $r-x_2$ diagrams.

Finally we show that a turning point in one of the fixed point branches causes a turning point in the *volume* vs. r diagram. The *volume* is defined (see Eqs. 9, 10 and 23) as:

$$V = \det\begin{bmatrix} (\hat{x}_1^1 - \hat{x}_1^2) & (\hat{x}_1^3 - \hat{x}_1^2) \\ (\hat{x}_2^1 - \hat{x}_2^2) & (\hat{x}_2^3 - \hat{x}_2^2) \end{bmatrix} \tag{A12}$$

The *volume* is a scalar function of reflux ratio. Differentiating Eq. A12 with respect to r, we obtain:

$$\frac{dV}{dr}=\sum_{k=1}^{c}\sum_{i=1}^{c-1}\frac{\partial V}{\partial \hat{x}_i^k}\frac{d\hat{x}_i^k}{dr} \tag{A13}$$

or explicitly for ternary mixtures,

$$\frac{dV}{dr}=(\hat{x}_2^3-\hat{x}_2^2)\frac{d\hat{x}_1^1}{dr}-(\hat{x}_1^3-\hat{x}_1^2)\frac{d\hat{x}_2^1}{dr}-(\hat{x}_2^3-\hat{x}_2^1)\frac{d\hat{x}_1^2}{dr}$$
$$+(\hat{x}_1^3-\hat{x}_1^1)\frac{d\hat{x}_2^2}{dr}+(\hat{x}_1^1-\hat{x}_1^2)\frac{d\hat{x}_1^3}{dr}-(\hat{x}_2^1-\hat{x}_2^2)\frac{d\hat{x}_2^3}{dr} \tag{A14}$$

If, at a certain value of r, there is a turning point in one branch (say branch 3), and no turning points in either of the other branches, then

$$\frac{dV}{dr}=\text{const}_1+(\hat{x}_1^1-\hat{x}_1^2)\frac{d\hat{x}_1^3}{dr}-(\hat{x}_2^1-\hat{x}_2^2)\frac{d\hat{x}_2^3}{dr} \tag{A15}$$

where const_1 denotes the first four terms on the right side of Eq. A14. The value of const_1 is finite. From Eq. A9 we get:

$$\frac{dV}{dr}=\text{const}_1+\left[(\hat{x}_1^1-\hat{x}_1^2)+\frac{\phi_{1,1}^3-\phi_{2,1}^3}{\phi_{1,2}^3-\phi_{2,2}^3}(\hat{x}_2^1-\hat{x}_2^2)\right]\frac{d\hat{x}_1^3}{dr} \tag{A16}$$

and finally, from Eq. A10:

$$\frac{dV}{dr}=\text{const}_1-[(\phi_{1,2}^3-\phi_{2,2}^3)(\hat{x}_1^1-\hat{x}_1^2)$$
$$+(\phi_{1,1}^3-\phi_{2,1}^3)(\hat{x}_2^1-\hat{x}_2^2)]\frac{1}{\det \boldsymbol{J}_\phi} \tag{A17}$$

Denoting the term in square brackets as const_2 we obtain:

$$\frac{dV}{dr}=\text{const}_1+\frac{\text{const}_2}{\det \boldsymbol{J}_F} \tag{A18}$$

At a turning point $\det \boldsymbol{J}_F=0$ and $(dV/dr)\to\infty$, provided that $\text{const}_2\neq 0$. Therefore, provided $\text{const}_2\neq 0$, a turning point in one of the fixed-point branches produces a turning point in the graph of *volume* vs. r. In all the examples we have studied, the numerical value of const_2 was nonzero at turning points in the fixed-point branches.

Manuscript received Feb. 27, 1991, and revision received Oct. 24, 1991.